

AD-A074 437

LITTON SYSTEMS INC  
DESIGN STUDY.(U)  
AUG 78

SAN CARLOS CALIF ELECTRON TUBE DIV

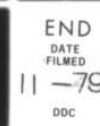
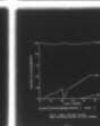
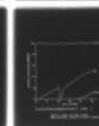
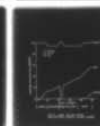
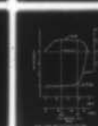
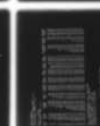
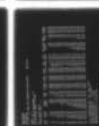
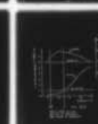
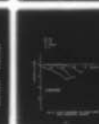
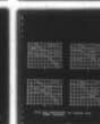
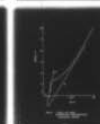
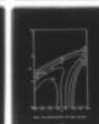
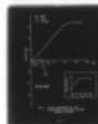
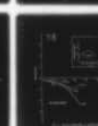
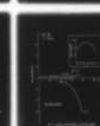
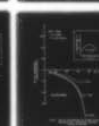
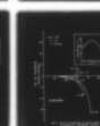
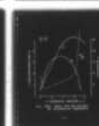
F/6 9/1

UNCLASSIFIED

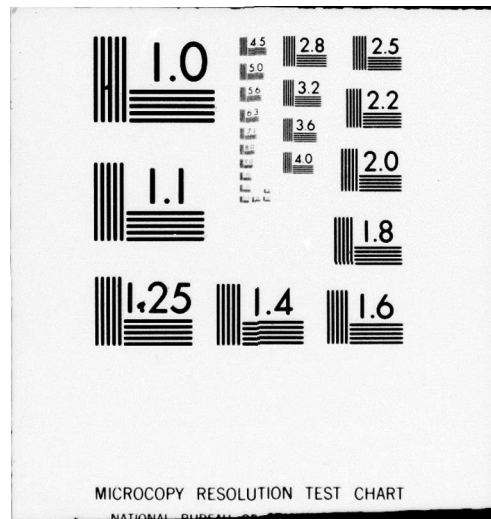
N00173-78-C-0428

NL

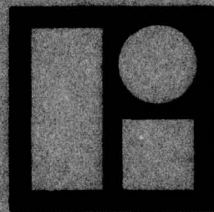
1 OF 1  
ADA  
074437



END  
DATE  
FILMED  
11 -79  
DDC



23720A



Litton

**ELECTRON TUBE DIVISION**

79 09 4 066

ADA074437

DDC ACCESSION NUMBER



DATA PROCESSING SHEET

PHOTOGRAPH THIS SHEET



Design Study, Final Rpt., Dtd. 15 Aug. 1978  
Contract No. N00173-78-C-0428

DOCUMENT IDENTIFICATION

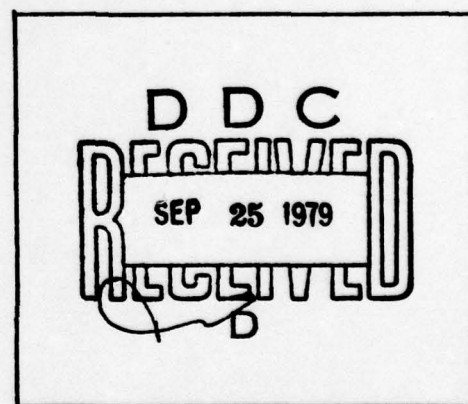
DISTRIBUTION STATEMENT A

Approved for public release;  
Distribution Unlimited

DISTRIBUTION STATEMENT

Accession For	
NTIS GRA&I	<input checked="" type="checkbox"/>
DDC TAB	<input type="checkbox"/>
Unannounced	<input type="checkbox"/>
Justification	
By <u>Per Htr. on file</u>	
Distribution/	
Availability Codes	
Dist.	Avail and/or special
<u>A</u>	

DISTRIBUTION STAMP



DATE ACCESSIONED

79 09 4 066

DATE RECEIVED IN DDC

PHOTOGRAPH THIS SHEET

AND RETURN TO DDA-2



DESIGN STUDY  
FINAL REPORT

Contract N00173-78-C-0428

LITTON SYSTEMS, INC.  
dba Litton Industries, Inc.  
960 Industrial Road  
San Carlos, California 94070

Prepared For:  
Naval Research Laboratory  
Code ~~5746~~<sup>5208</sup>/R. Van Wagoner  
Washington, D.C. 20375

August 15, 1978

## TABLE OF CONTENTS

<u>Section</u>	<u>Title</u>	<u>Page</u>
1.0	SUMMARY AND RISK ANALYSIS	1
2.0	EVALUATION OF THE MECHANICAL AND ELECTRICAL FEATURES WHICH LIMIT THE ATTAINMENT OF THE LOW AM-PM CONVERSION DESIRED IN A TWT WITH THE SPECIFIED BANDWIDTH AND OUTPUT POWER	7
2.1	The Synchronism Parameter - b	11
2.2	The Space Charge Parameter - QC	24
2.3	The Loss Parameter - d	28
3.0	DEVELOPMENT OF DESIGNS WHICH COULD SATISFY THE DESIRED SPECIFICATION	32
3.1	Design I -- Wideband Circuit, Loss-Button Stabilized	32
3.2	Design II -- Wideband Circuit, Lossy-Line Stabilized	40
4.0	REFERENCES	58

### LIST OF FIGURES

<u>Figure No.</u>	<u>Title</u>	<u>Page</u>
1	L-5388, S7N 2015 AM-PM Vs. Frequency Sat. Power Vs. Frequency	3
2	L-5511, S/N 2007 AM-PM Vs. Frequency Sat. Power Vs. Frequency	4
3	L-5631 Data @ 31.5 kV, 6A (DC-200)	6
4a	Phase Deviation Vs. Drive Power	8
4b	AM-PM Conversion Vs. Drive Power	8
5	Small Signal Gain & Efficiency Vs. Synchronism Parameter b	12
6	AM-PM Conversion Vs. Power Output Synchronism Parameter Variable (Midband)	14
7	AM-PM Conversion Vs. Power Output Synchronism Parameter Variable (Lower Bandedge) ..	15
8	AM-PM Conversion Vs. Power Output Synchronism Parameter Variable (Upper Bandedge) ..	16
9	AM-PM Conversion Vs. Power Output Synchronism Parameter Variable (Lower Bandedge) ..	18
10	AM-PM Conversion Vs. Power Output Synchronism Parameter Variable (Upper Bandedge)	19
11	AM-PM Conversion Vs. $\eta/C$ Synchronism Parameter Variable (Lower Bandedge)	20
12	AM-PM Conversion Vs. $\eta/C$ Synchronism Parameter Variable (Upper Bandedge)	21
13	Data From Ezura and Kono	22
14	Optimum AM-PM Conversion Vs. Frequency	23
15	Gain Characteristics for Optimum Circuit	25



LIST OF FIGURES (cont'd)

<u>Figure No.</u>	<u>Title</u>	<u>Page</u>
16	Gain Characteristics For L-5631, S/N 2001	26
17	L-5631, S/N 2001 Dispersion Characteristics (Unloaded Circuit)	27
18	Gain Characteristics for Variable Space Charge Parameter	29
19	AM-PM Conversion Vs. Power Output Loss Parameter Variable	30
20	L-5388, S/N 2015 AM-PM Vs. Frequency Sat. Power Vs. Frequency	33
21	L-5511, S/N 2007 AM-PM Vs. Frequency Sat. Power Vs. Frequency	34
22	E-W Tube - Design 1	36
23	Transmission Characteristics for E-W Tube	38
24	L-5631 Data @ 31.5 kV, 6A (DC-200)	47
25	Loss-Line Pole Piece Construction	49
26a	High "Q" Loss Line Construction (Upper Cutoff)	50
26b	Low "Q" Loss Line Construction (In-Band)	50
27	Return Loss and Insertion Loss for the Output Section at L-5631, S/N 2001	52
28	L-5631 Circuit Layout	53
29	L-5631, S/N 2001 - 7.5 GHz Gain, Efficiency Velocity, Vs. Cavity Number	55
30	L-5631, S/N 2001 - 9.0 GHz Gain, Efficiency, Velocity, Vs. Cavity Number	56
31	L-5631, S/N 2001 - 10.5 GHz Gain, Efficiency, Velocity, Vs. Cavity Number	57



LIST OF TABLES

<u>Table No.</u>	<u>Title</u>	<u>Page</u>
1	Chosen Design Parameters	39
2	VA118A - 15 GHz	41
3	VA118B - 15 GHz	42
4	VA118A - 16 GHz	43
5	VA118B - 16 GHz	44
6	VA118A - 17 GHz	45
7	VA118B - 17 GHz	46

## 1.0 SUMMARY AND RISK ANALYSIS

This study shows that low AM-PM conversion can be obtained over a wide instantaneous bandwidth by using a broadband circuit with the proper dispersion characteristics. Circuits having the prescribed characteristics have been used for several years in high power coupled cavity tubes at Litton Industries. The circuits were not developed to provide low AM-PM but to provide high power operation over wide bandwidths. The low AM-PM characteristics are an additional attribute discovered quite accidentally. This study shows why tubes using these circuits have the low AM-PM conversion demonstrated. Although the study utilized an X-band circuit (7.0 to 11.0 GHz) the results are applicable in other frequency bands. The circuit can be scaled directly so that the values of phase velocity and impedance are the same. The loss parameter, which increases at higher frequencies due to skin effect losses, can be decreased by choosing a solenoid design which utilizes an all OFHC copper circuit to minimize losses.

The study shows how the tube parameters  $b$ ,  $QC$ , and  $d$  affect AM-PM conversion. An understanding of the effects of these parameters is essential in designing low AM-PM tubes. The lossy line tube data presented in Figure 3 shows considerable progress in improving the AM-PM performance of the wideband family of tubes. The very long output section used in this tube provides sufficient small signal gain even at 10.0 GHz to produce high saturated power and low AM-PM conversion. Comparison with Figure 1 for the comparable loss button tube shows just how important the long output section is. Further improvements yet may be obtained using even longer output section lengths. More sophisticated loss patterns can be used now that the basic design procedures have been proven sound.



Two preliminary designs which can satisfy the desired specifications are proposed. In Sections 3.1 and 3.2 these designs are presented in detail. In this section, we shall summarize both designs and make recommendations.

#### Design 1 -- Wideband Circuit, Loss Button Stabilized

This circuit would be scaled from our present wideband button stabilized family of tubes. Figures 1 and 2 show the power output and AM-PM characteristics from representative samples of these tubes. The specified band is shown scaled to an appropriate frequency region over which the power output and AM-PM requirements are met. Note that the band is oriented near the lower band edge of hot tube bandwidths. It has been shown in Section 2 that the best AM-PM characteristics are found at the low frequency end of the band. The proper scaling then leads to a hot tube bandwidth of 14 - 22 GHz for this tube. The scale factor from the present L-5511 Ku-Band tube is .785:1.

The design details for this tube are presented in Section 3.1. The gun design has been completed and a modified L-5511 gun will be used. The collector will also be the L-5511 collector.

The risk associated with this design is the minimum of the two final designs. The gun design is completed. The solenoid design is straight-forward so the focusing problems are well in hand. The loss button technology for stabilization is the standard by which all production coupled cavity tubes are built. The circuit is a direct scale from those used successfully in production tubes.

The only problems will be associated with the higher frequency high end of the tube. The L-5511 window design will have to be modified to provide a good match up to about 20 GHz beyond which with sufficient loss will be used to stabilize the high end of the tube.

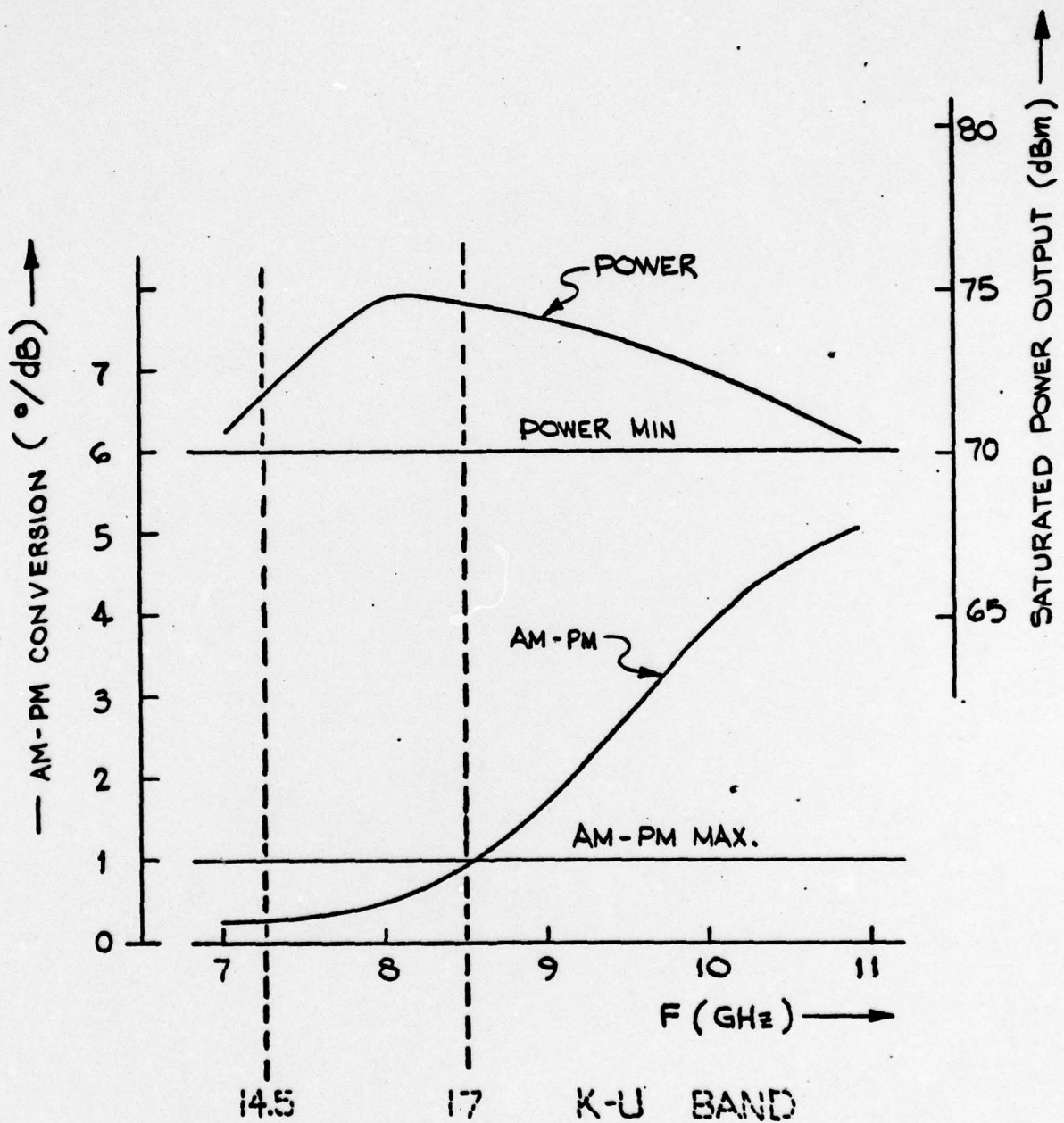


FIG. 1 L-5388 9/N 2015  
 AM-PM VS FREQUENCY  
 SAT. POWER VS FREQUENCY



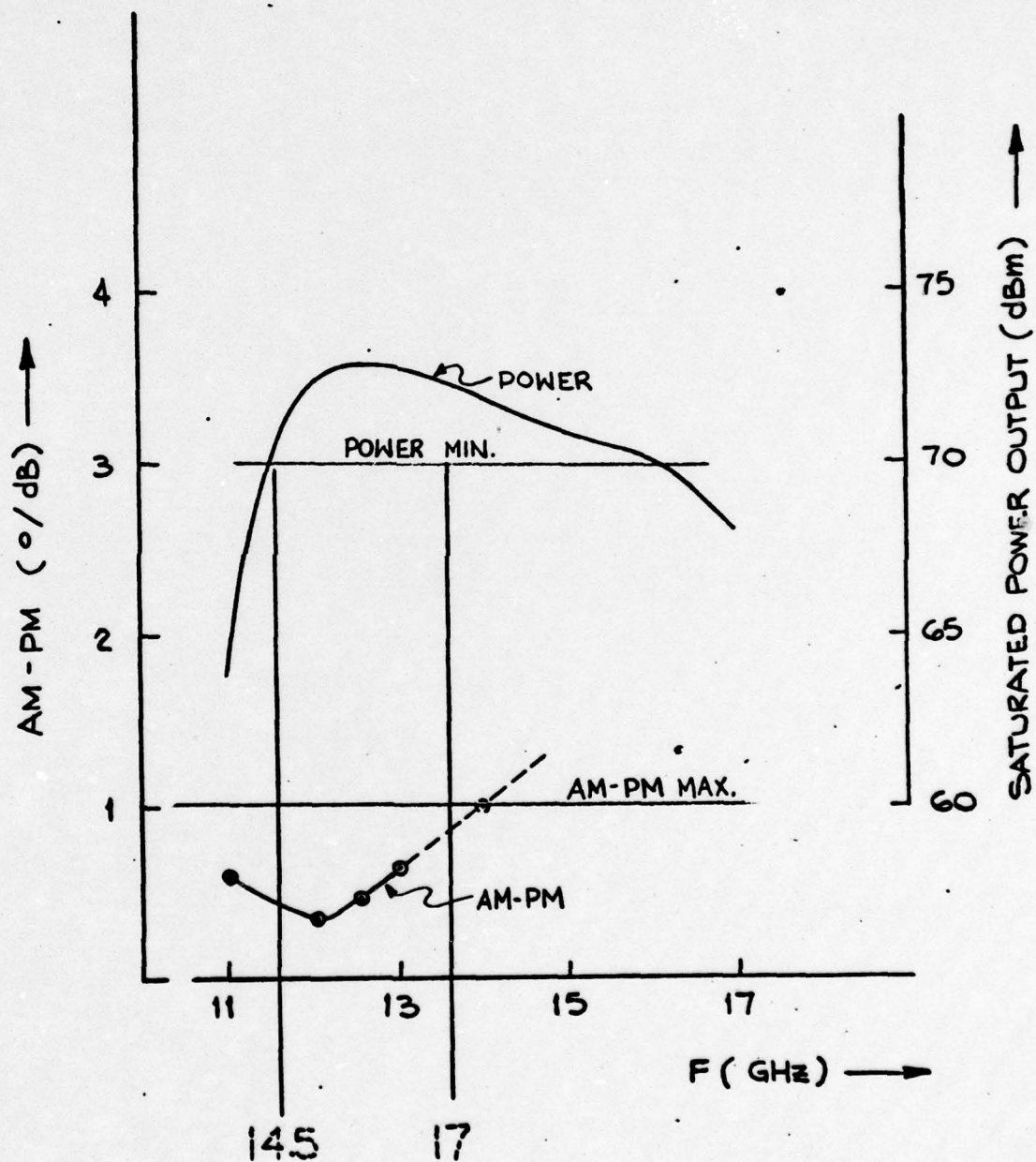


FIG. 2 L-5511 9/N 2007  
 AM-PM VS FREQUENCY  
 SAT. POWER VS FREQUENCY

## Design 2 -- Wideband Circuit, Lossy-Line Stabilized

The circuit for this design would be scaled from the I-Band lossy-line tube, the L-5631, S/N 2001. The hot bandwidth would be 12.0 - 18.9 GHz. The frequency of 12.0 GHz corresponds to 7.0 GHz and 18.9 GHz corresponds to 11.0 GHz. This scale factor is .585:1.

Figure 3 shows the saturated output power and AM-PM data from the L-5631 S/N 2001. Superimposed on this data are the projected Ku-Band scaled frequencies. The purpose of this figure is to show the relative orientation of the objective band with relation to the full hot band of the tube. Note that the 14.5 - 17 objective band has been oriented nearer the high end of the hot band than in Design 1. This is possible because the AM-PM characteristics are better for the lossy-line stabilized tube. It is advantageous because:

- 1) The size of the circuit is maximized making it easier to build and capable of higher average power,
- 2) The similarity is very close to the present 11 - 17 GHz Navy J-Band in that the gun, windows and collector may all be directly used on this tube, and
- 3) The future potential for a full 12 - 18 GHz low AM-PM tube is very good with some improvements in the output section of the tube to extend the present performance to 18 GHz.

The main problem will arise in implementing the lossy-line technology at Ku-Band where the small sizes will make fabricating difficult. Some redesign of the lossy-line assemblies will be necessary to overcome structural difficulties.

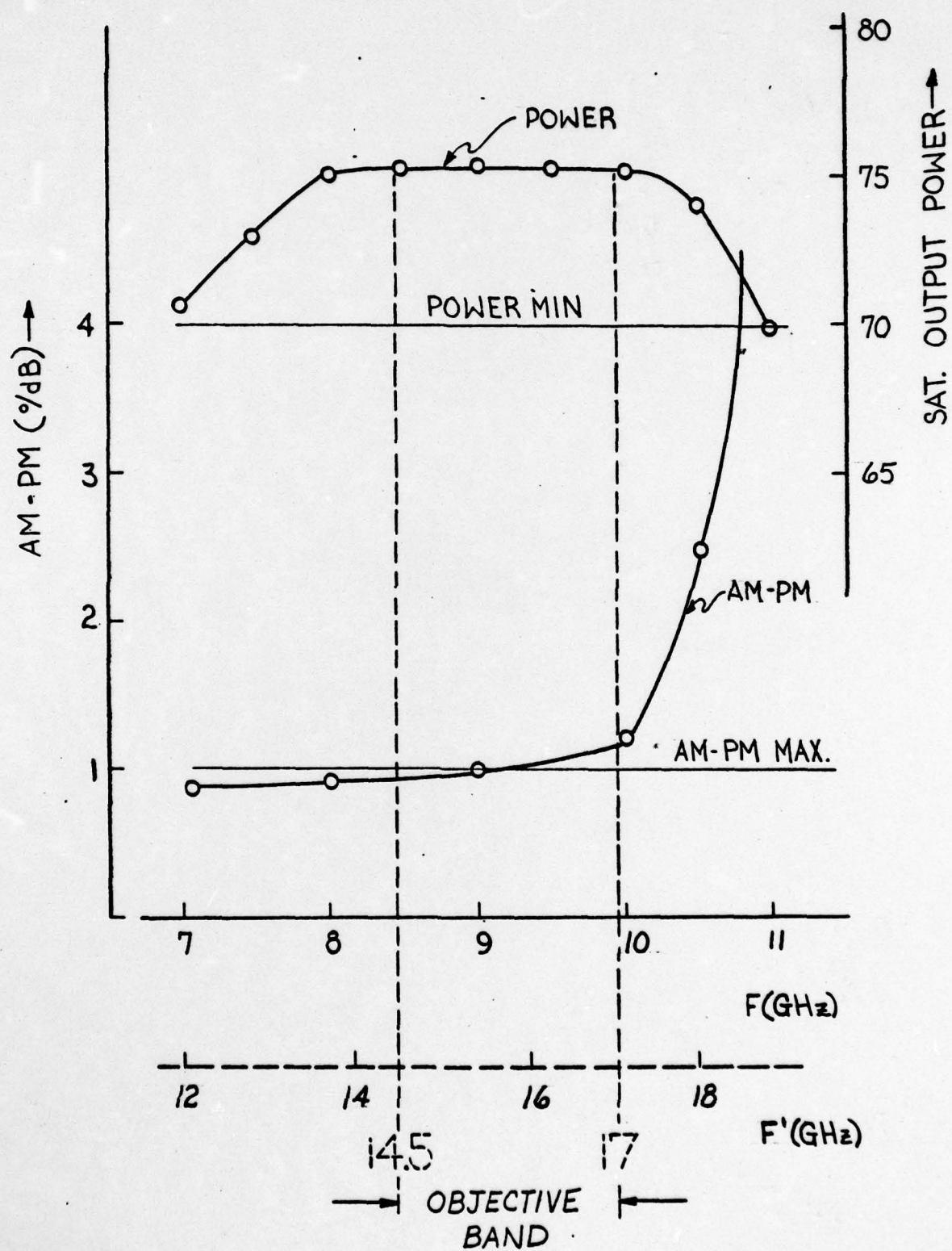


FIG. 3 L-5631 DATA @ 31.5 KV, 6A (DC-200)



## 2.0 EVALUATION OF THE MECHANICAL AND ELECTRICAL FEATURES WHICH LIMIT THE ATTAINMENT OF THE LOW AM-PM CONVERSION DESIRED IN A TWT WITH THE SPECIFIED BANDWIDTH AND OUTPUT POWER

---

The problem of minimizing AM-PM has been studied both by reviewing past efforts reported in the literature and by means of large signal computer runs. The results of the work are discussed in this section.

AM-PM conversion is defined as the rate of change of output phase with respect to an amplitude change of input RF power. It is normally defined at saturation since this is where most radar tubes are operated, but the definition can be used in a broader sense over the full drive power range. Figure 4 shows the relative phase deviation from small signal and AM-PM conversion as a function of drive power for a typical TWT. In the small signal region both the phase output deviation  $\Delta\phi$  and the AM-PM conversion are small. As the tube is driven into large signal operation the phase deviation increases and the AM-PM conversion increases. An average AM-PM conversion could be defined as  $\Delta\phi/\Delta P_{in}$ .  $\Delta\phi$  is the total phase deviation from small signal to saturated large signal operation and  $\Delta P_{in}$  is the corresponding range of input power. Note that in Figure 4b the AM-PM conversion actually reaches a peak before saturation. It should be mentioned that this figure, although typical, does not represent all cases. In some cases the peak AM-PM occurs at saturation or beyond and may be positive or negative. Indeed the phenomena is very complex; the long list of references at the end of this report shows a good number of researchers have studied the problem.

Beam et al<sup>6</sup> derived a relationship which predicts phase deviation in TWTs to first order. They found that phase output in the case



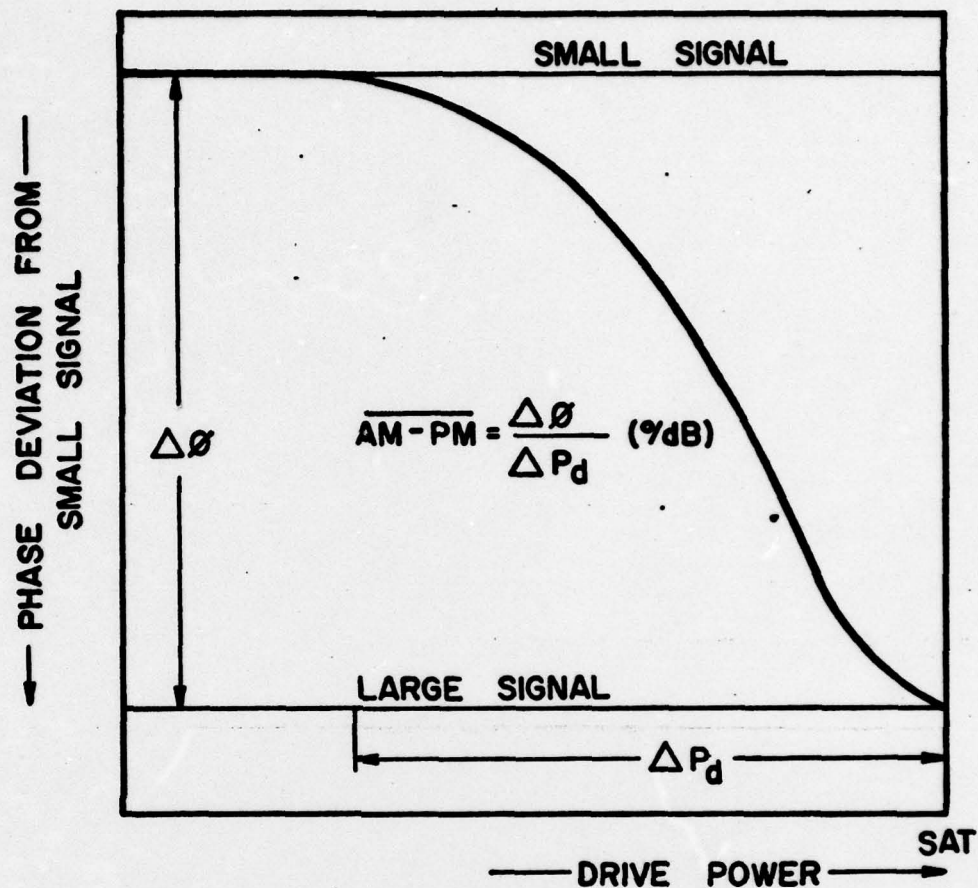


FIG.4a PHASE DEVIATION VS. DRIVE POWER

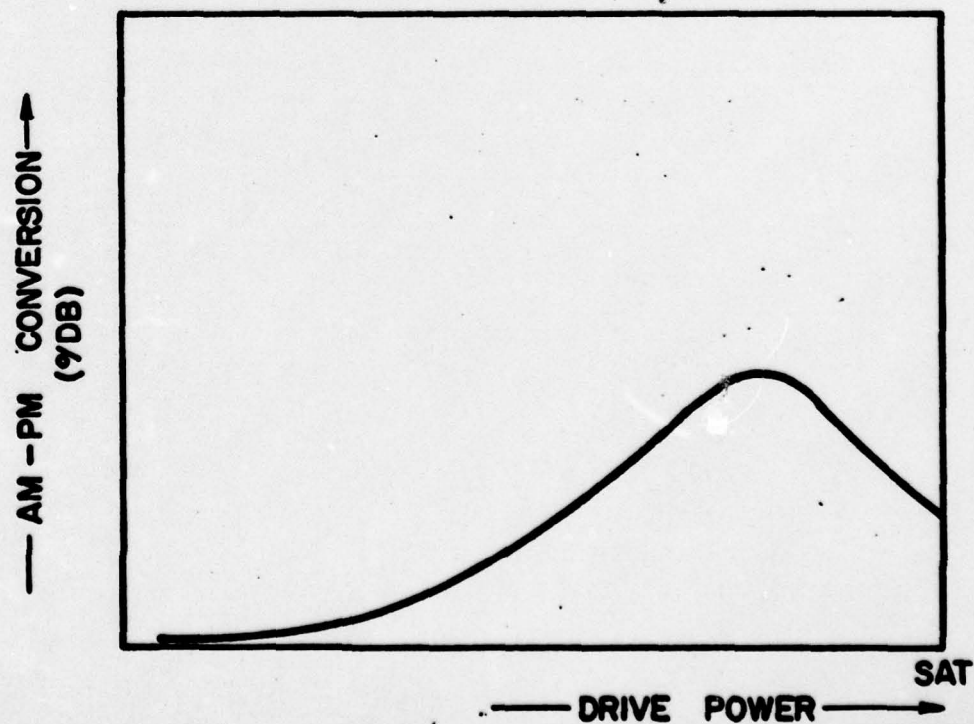


FIG.4b AM-PM CONVERSION VS. DRIVE POWER

of large signal operation deviates from that in the use of small signal operation by:

$$\Delta\phi = K \times \frac{P_o}{P_{dc}} \times \frac{1}{C} \text{ degrees}$$

where  $\Delta\phi$  = the phase deviation

$P_o/P_{dc}$  = the electronic efficiency

$C$  = Pierce's gain parameter

$K$  = a constant

The implication of this formula is that the phase deviation can be reduced by maximizing the gain parameter,  $C$ , and minimizing the electronic efficiency.

An heuristic explanation for the phase deviation is that in the saturation region the electron beam transfers energy to the circuit and in so doing slows down. The phase relationship between the beam and circuit waves which existed in the small signal region is changed and the difference is integrated over the saturation region of the tube. Obviously the lower the electronic efficiency is, the less the beam slows down and the lower the total phase deviation is. Also the higher the gain the shorter in length is the saturation region and the integrated effect is less.

Beam<sup>6</sup> concluded that the best way to minimize the phase deviation at high power levels was to "make the power-handling capacity so great that the maximum output power will be less than 1 per cent of the beam power".

One way then to achieve the required AM-PM conversion would be to operate the tube in the small signal region. To achieve a 10 kW output power a 200 kW saturated tube would have to be designed. Even with solenoid focusing a design over the required bandwidth would lead to quite impractical thermal requirements on the slow-wave structure. The requirement for a gridded gun is particularly difficult, since the focusing is not nearly as good for

a gridded gun as for cathode pulsed operation. Another problem of operating the tube in the small signal region is that of considerable gain and power variation over the required bandwidth.

There are other tube factors which also influence  $\Delta\phi$  such as synchronism parameter  $b$ , the space charge parameter  $QC$ , and the loss parameter  $d$ . Other researchers<sup>11, 12, 17</sup> have measured AM-PM and discovered some important second order effects. In particular, they find that undervoltaging the tube (that is, operating the tube at a voltage less than that voltage which produces maximum small signal gain) reduces AM-PM at the same output power level. Linstrom<sup>12</sup> reports measurements that show minimum AM-PM when operating at a beam voltage 4% lower than the corresponding to the maximum small signal gain. In addition, he measures negative as well as positive phase deviation, an impossible result from the Beam theory. Both Ober<sup>11</sup> and Nishihara<sup>17</sup> verify with measurements that positive and negative phase deviation exists. The question then arises whether or not there exists a value of synchronism parameter  $b$  at which the phase deviation is exactly zero. Such a value is theoretically predicted by Nilsson<sup>13</sup>. Ober<sup>11</sup> postulates that in addition to the positive component of phase deviation due to loss of beam kinetic energy that there is a negative component due to nonlinear beam modulation, and that it should be possible to make a tube in which "the negative and positive components cancel each other so that the AM-PM conversion becomes very small". Ober's experimental tubes showed AM-PM conversion measurements of less than  $1^\circ/\text{dB}$  at saturation at an optimum value of  $b$  which calculates to be about  $.95 X_1$ , where  $X_1$  is the maximum small signal gain parameter.

We have investigated the dependence of AM-PM conversion on the tube parameters  $b$ ,  $QC$  and  $d$  using a large signal computer program. This computer program was written by Dr. J. R. M. Vaughan of Litton Industries. The program in general works quite well in modeling tubes up to saturation, but does not work satisfactorily beyond saturation in the overdrive region. We are, however, most



interested in studying the near saturation region where the nonlinearity process begins and, therefore, the program is adequate. We have run some test cases to verify that the program agrees with measurements made on production tubes. The 12-disk model runs well qualitatively, but gives results about a factor of 2 higher than measurements. The 24-disk model is closer, but is of course more expensive to run. We have used the 12-disk model in the early exploratory work for economy and then used the 24-disk model for further refinements.

## 2.1 The Synchronism Parameter - $b$

The synchronism parameter,  $b$ , is a measure of the velocity difference between the electron beam and the slow-wave structure.  $b = 0$  represents "synchronism" when the beam velocity and circuit velocity are the same. Positive  $b$  means the beam travels faster than the circuit.

Figure 5 shows how the tube efficiency, gain per wavelength, and the ratio of  $\eta/G\lambda$  vary with  $b$ . The efficiency and gain per wavelength do not maximize at the same value of  $b$ . Tubes are generally designed to operate at the maximum efficiency. The length of the tube is adjusted to meet the gain requirement. The ratio of efficiency to gain per wavelength has been shown earlier to be proportional to the phase deviation. Consider the case when the tube is overvoltaged; that is,  $b$  is greater than  $b_0$  the value of  $b$  for maximum small signal gain (in this case  $b = 1$ ). The efficiency is high and the gain per wavelength is reduced from its maximum value. Thus the distortion is high. The greater the overvoltaging the higher the distortion. As the cathode voltage is reduced, the efficiency falls off while the gain per wavelength first increases to its maximum and then decreases slowly. The distortion then decreases as shown until the gain falls off faster than efficiency, at which point the minimum distortion has been reached. Of course the situation is a bit more complicated as the computer results will show.



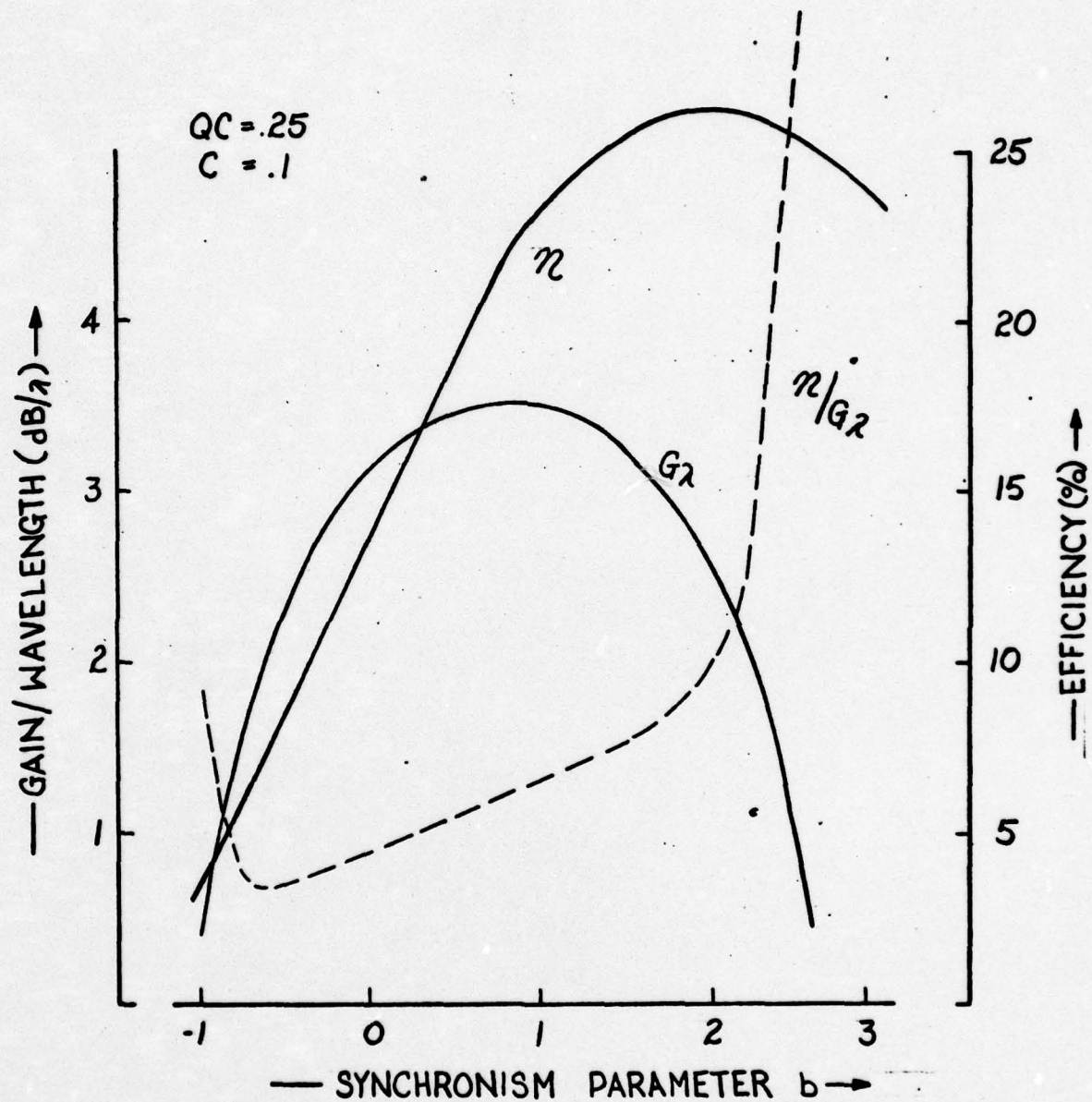


FIG. 5 SMALL SIGNAL GAIN AND EFFICIENCY  
 VS. SYNCHRONISM PARAMETER  $b$

For the computer model a hypothetical tube was analyzed which had no attenuator or sever to avoid complicating the results. The phase velocity of the circuit was varied artificially without changing any other parameter; thus the input power  $P_{dc}$  was constant, the cathode voltage  $V_c$ , and cathode current  $I_c$  were constant, the circuit parameters  $K_0$ ,  $\alpha_0$ ,  $r_0$  were constant.  $K_0$  is the interaction impedance,  $\alpha_0$  is the circuit attenuation and  $r_0$  is the tunnel radius. For each value of phase velocity there was then a unique value of  $b$ . The drive power was varied in setps from a low level corresponding to an electronic efficiency of about .1% to saturation efficiency. From this data Figure 6 was constructed. In this figure AM-PM conversion is plotted as a function of output power. Obviously for low output power ( $< 60$  dBm) the AM-PM conversion is low. For high values of  $b$  ( $b > 2.0$ ) and low values of  $b$  ( $b < .65$ ) corresponding to low gain (see gain vs.  $b$  chart in upper right corner of Figure 6) the AM-PM conversion is high. Low values of  $b$  also correspond to low efficiency. It is interesting to note that the computer program shows both positive and negative conversion. We did not find a value of  $b$  for which there was no phase deviation. We did find a range  $.95 \leq b \leq 1.5$  over which AM-PM was low. At  $b = 1.3$  the tube has 0 AM-PM at saturation at an output power of 74 dBm (25 kW) and an efficiency of 16%.

The computer study was continued to determine over how wide a bandwidth low AM-PM could be obtained at a single value of cathode voltage. The circuit we analyzed had a cold bandwidth from 7.2 GHz to 12.0 GHz. Computer runs were made at 7.5 GHz and 10.5 GHz to obtain the optimum value of  $b$  at these frequencies. The data is shown plotted in Figures 7 and 8 respectively.

*Explain why 7.2-12*

The data at 7.5 GHz (Figure 7) shows that quite low AM-PM levels may be obtained at this frequency. The optimum occurs between  $b = 0$  and  $b = .17$ . In Figure 8 the data at 10.5 GHz is plotted, the AM-PM minimum is around  $b = 1.36$  and the minimum value of AM-PM is higher than at midband.

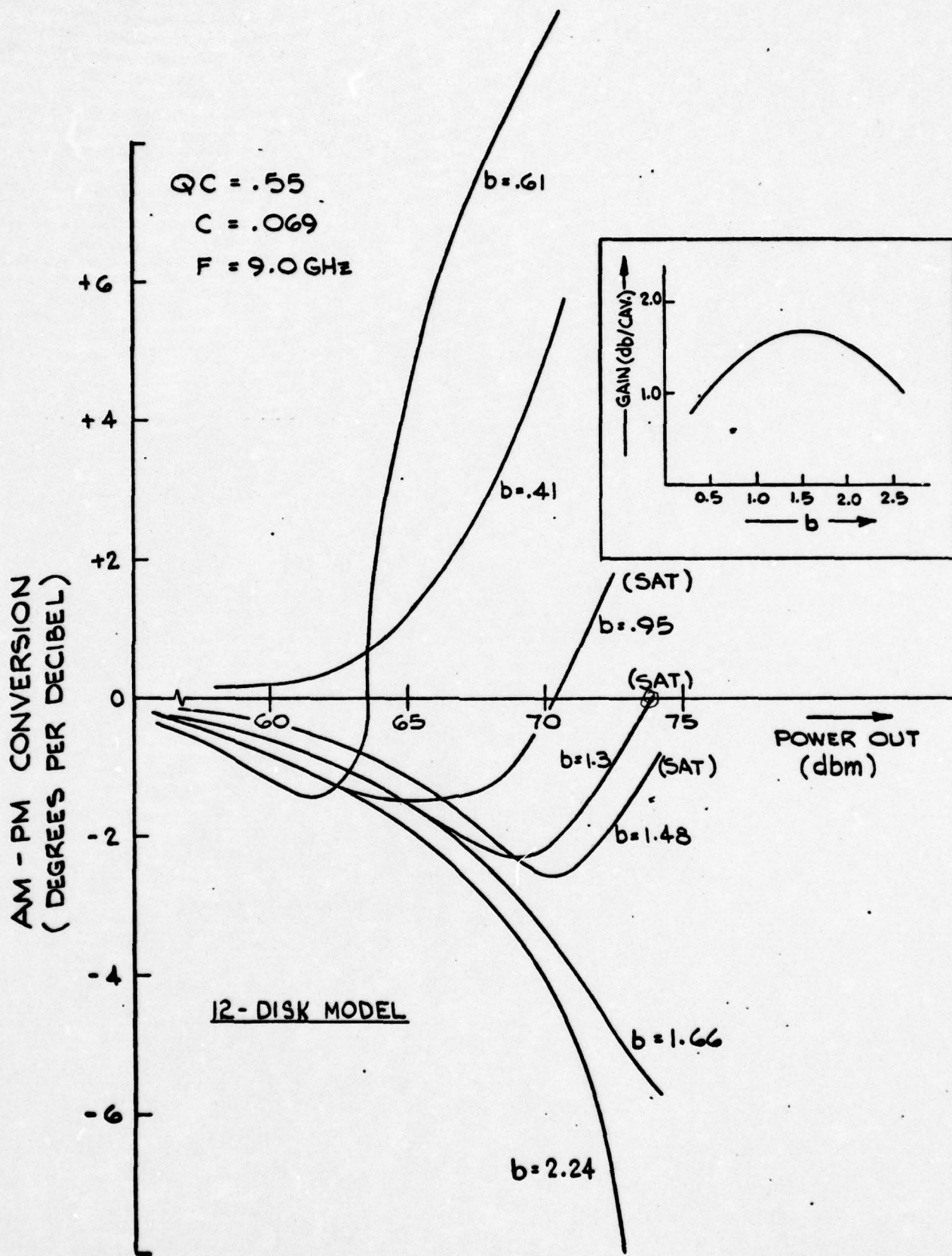


FIG. 6 AM-PM CONVERSION VS. POWER OUTPUT  
 SYNCHRONISM PARAMETER VARIABLE  
 (MIDBAND)



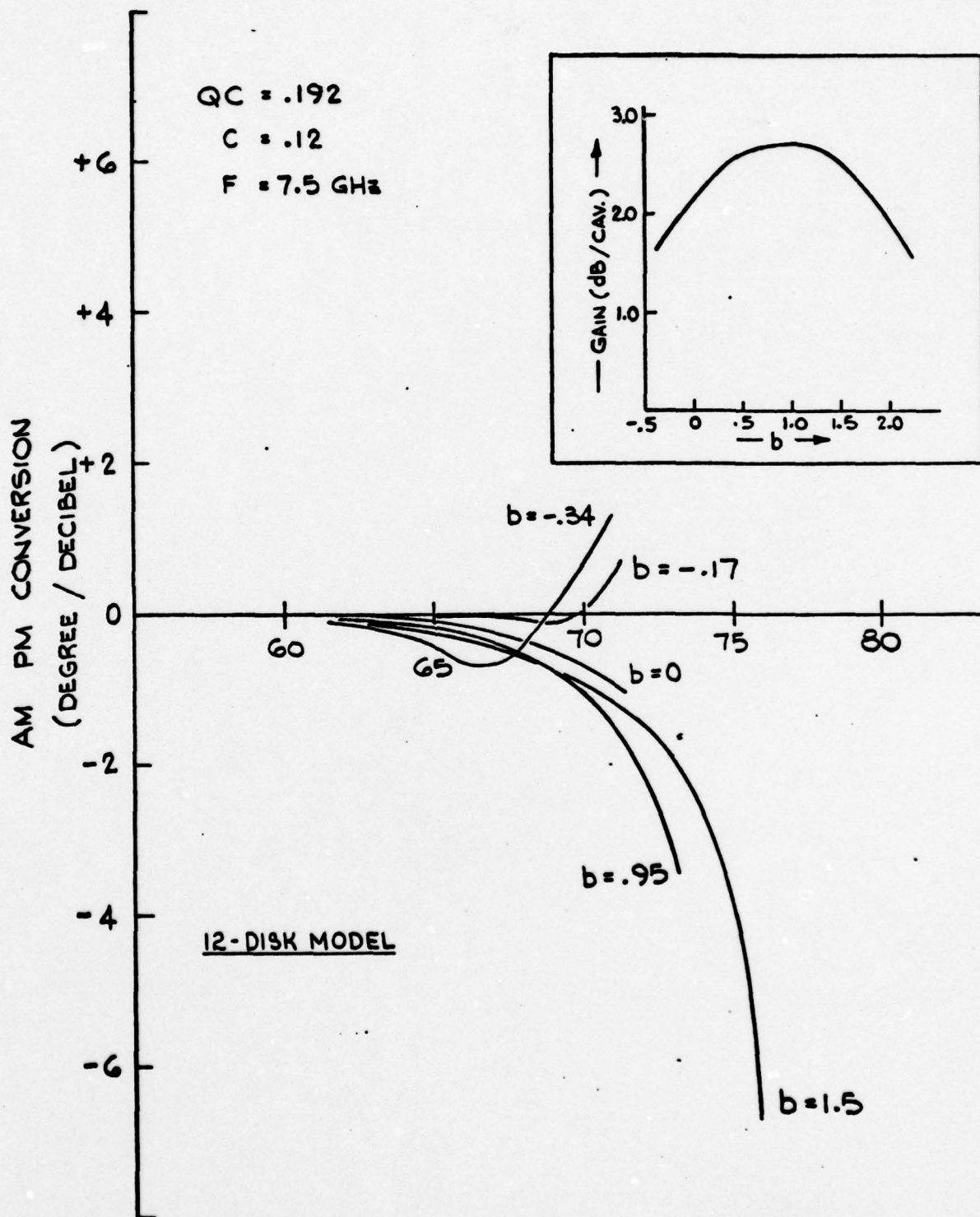


FIG. 7 AM-PM CONVERSION VS. POWER OUTPUT SYNCHRONISM PARAMETER VARIABLE (LOWER BANDEDGE)

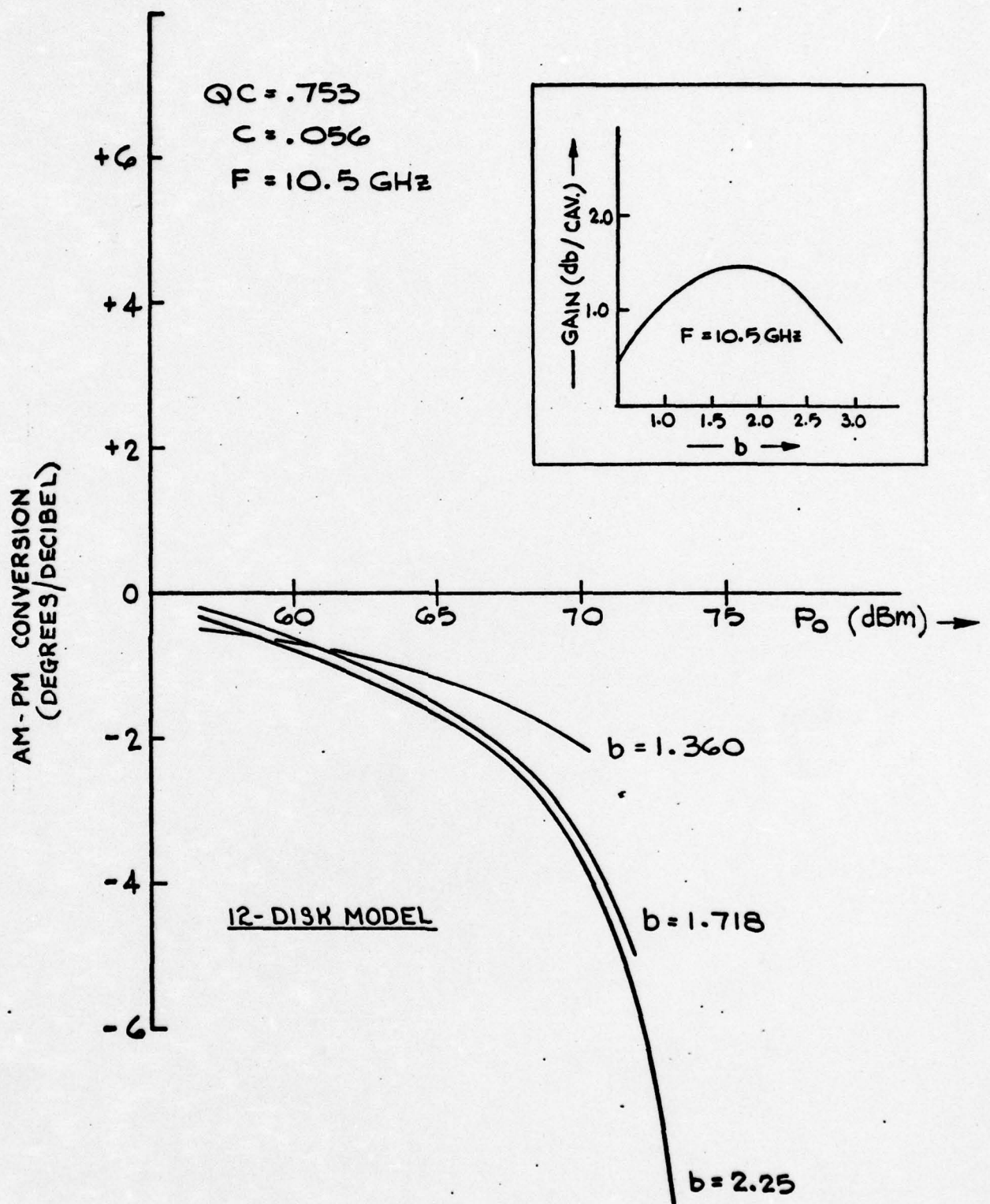


FIG. 8 AM-PM CONVERSION VS. POWER OUTPUT  
SYNCHRONISM PARAMETER VARIABLE  
(UPPER BANDEDGE)

Computer runs (24 disk model) were made at 7.5 GHz and 10.5 GHz using the same parameters to refine the 12 disk model runs.

Figure 9 shows the results of 24-disk model runs at 7.5 GHz plotted on the same scale as used on the 12-disk model runs. Comparing the 12 and 24-disk results shows good agreement with about the same quantitative results. The 24-disk runs show a slightly positive AM-PM conversion for low values of  $b$ .

Figure 10 shows the plotted results of the 24-disk model runs at 10.5 GHz. Again the 12 and 24-disk model results are similar with the 24-disk runs showing less AM-PM conversion which was consistently the case over the large number of runs made.

Figure 11 shows the same 24-disk data as in Figure 9 plotted to a different abscissa, namely  $\eta/C$ . This was done to compare the results with the work of Ezura<sup>21</sup>. The sign of the AM-PM conversion was also changed to agree with Ezura's convention. Figure 12 likewise shows the same data as Figure 10 plotted on the  $\eta/C$  scale. Figure 13 is data taken from Ezura's paper. Comparing Figures 11, 12 and 13 substantially the same kind of results are seen. As the synchronism parameter  $b$  is decreased, the AM-PM conversion becomes smaller. The range of AM-PM and  $\eta/C$  compare well with our results as well. Ezura's calculated data comes from a Lagrangian large signal theory, a method quite different from the one we are employing.

The optimum values of AM-PM at 7.5, 9.0 and 10.5 GHz are shown plotted in Figure 14. Note that the best results were obtained at the low frequency end of the hot bandwidth. These values are the best AM-PM that can be achieved at any value of cathode voltage and they do not include the effects of attenuators or an output section that is too short.



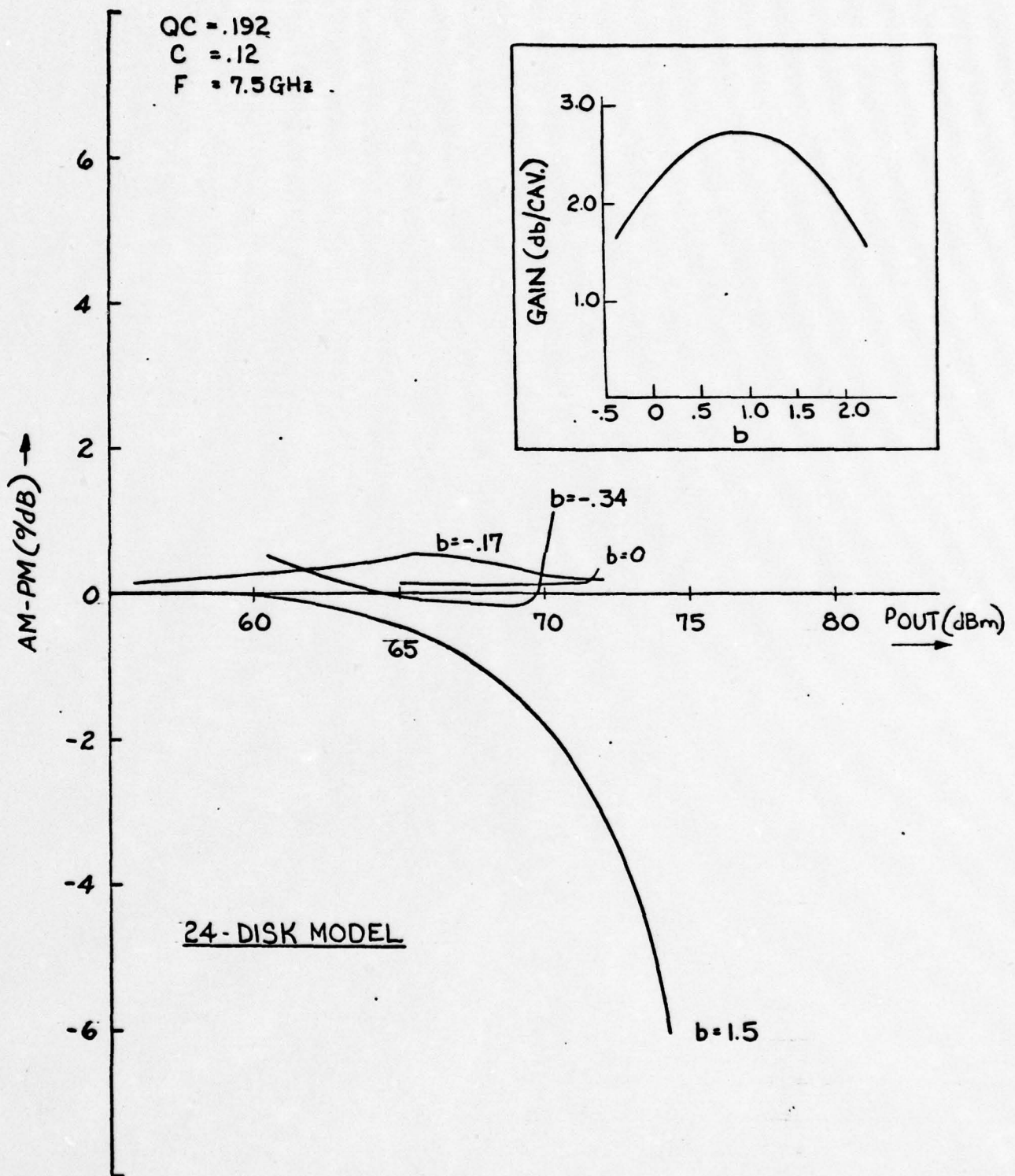


FIG. 9 AM-PM CONVERSION VS. POWER OUTPUT  
SYNCHRONISM PARAMETER VARIABLE.  
(LOWER BONDEDGE)

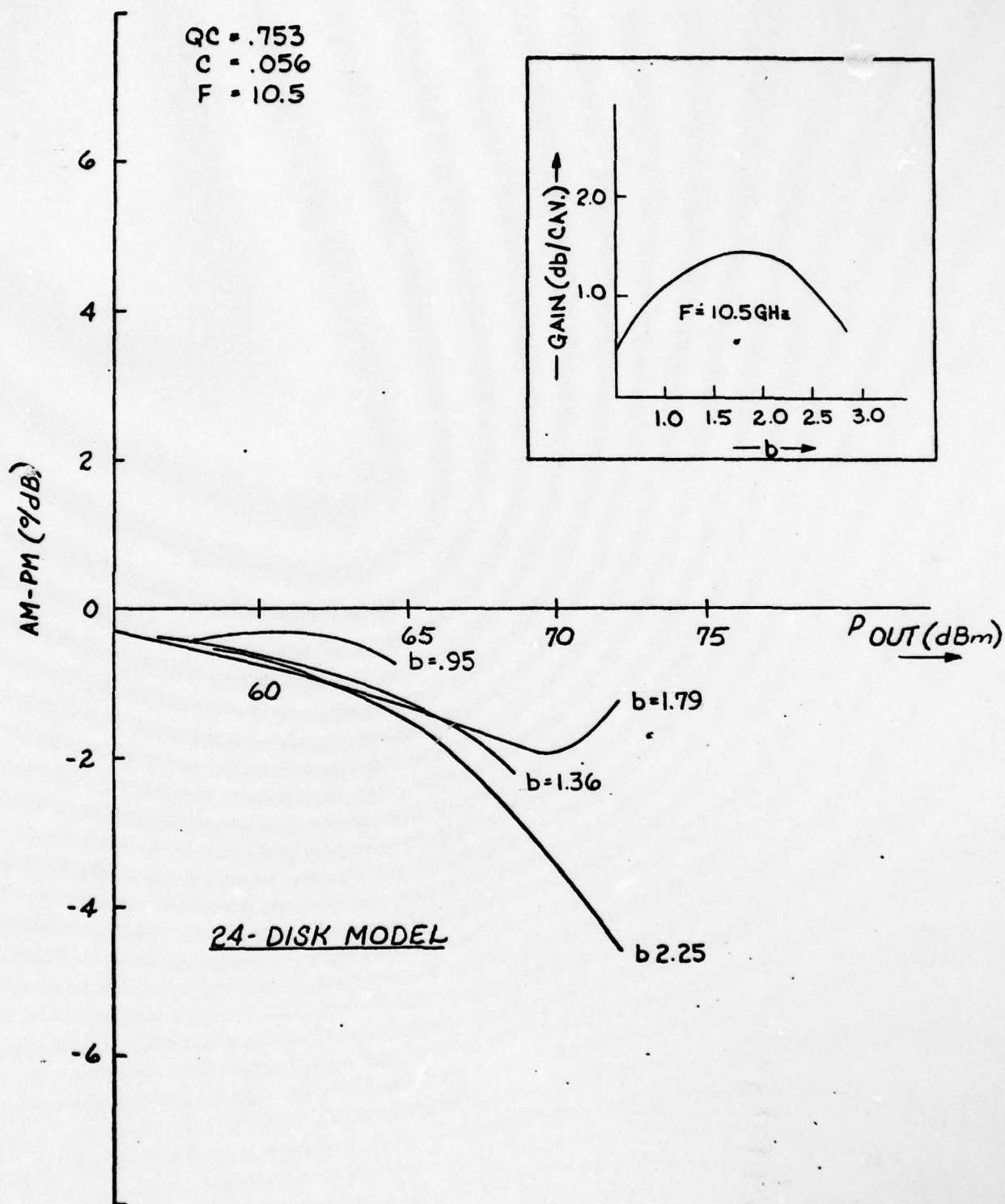


FIG. 10 AM-PM CONVERSION VS. POWER OUTPUT  
SYNCHRONISM PARAMETER VARIABLE.  
(UPPER BOND EDGE)

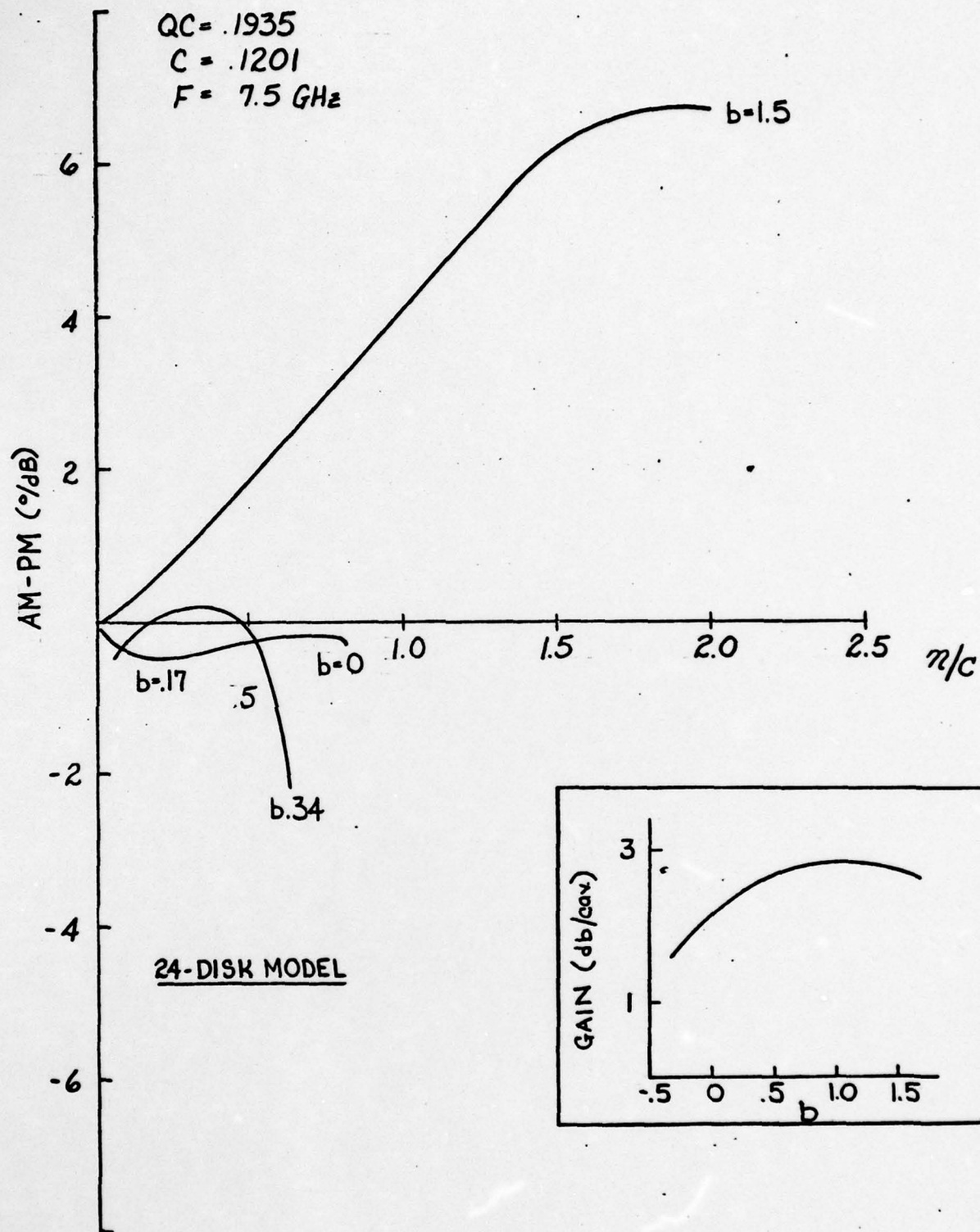


FIG. 11 AM-PM CONVERSION VS  $\pi/c$   
 SYNCHRONISM PARAMETER VARIABLE.  
 (LOWER BANDEDGE)



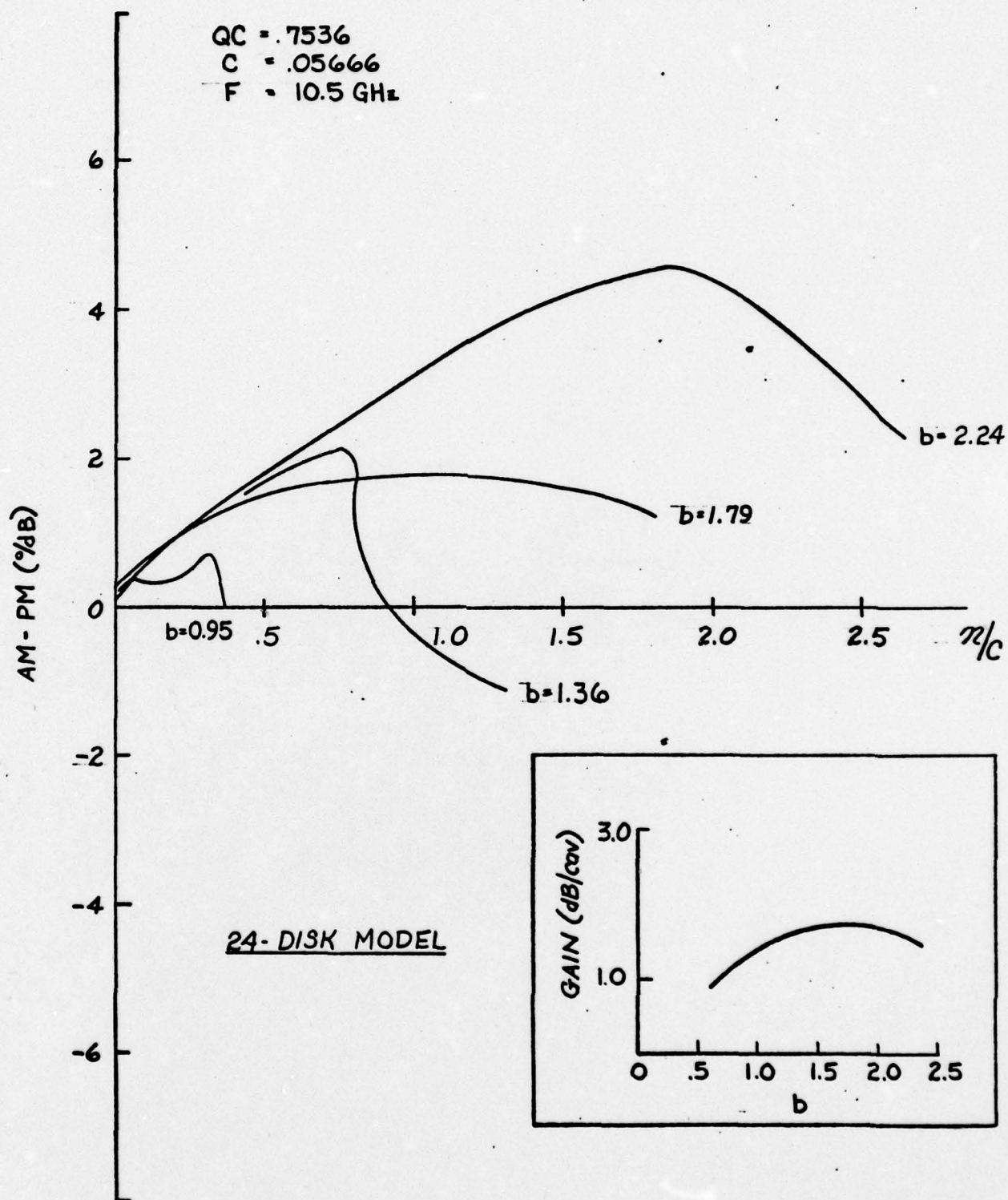


FIG. 12 AM-PM CONVERSION VS.  $\pi/c$   
 SYNCHRONISM PARAMETER VARIABLE.  
 (UPPER BANDEDGE)

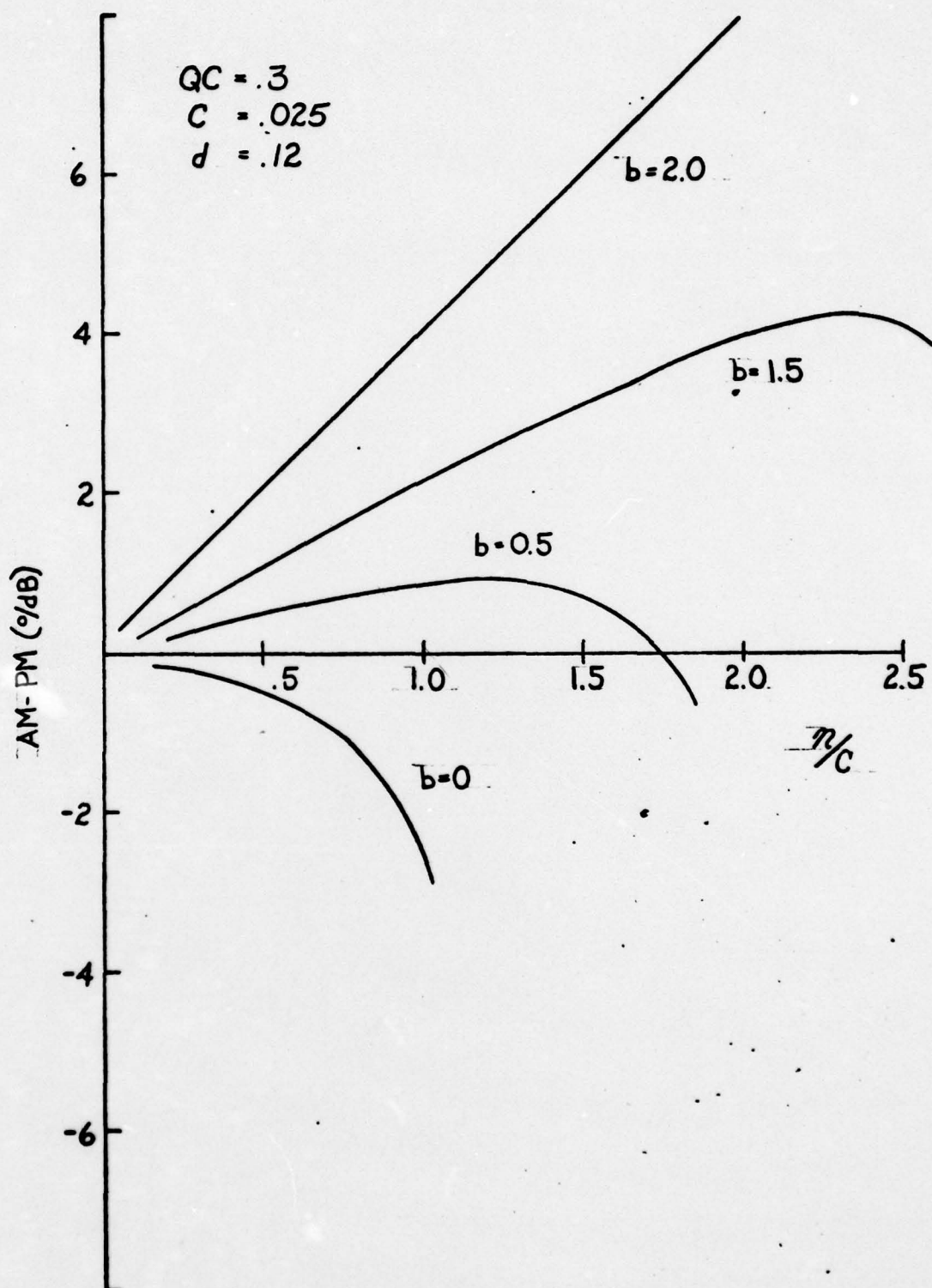


FIG. 13 DATA FROM EZURA AND KANO

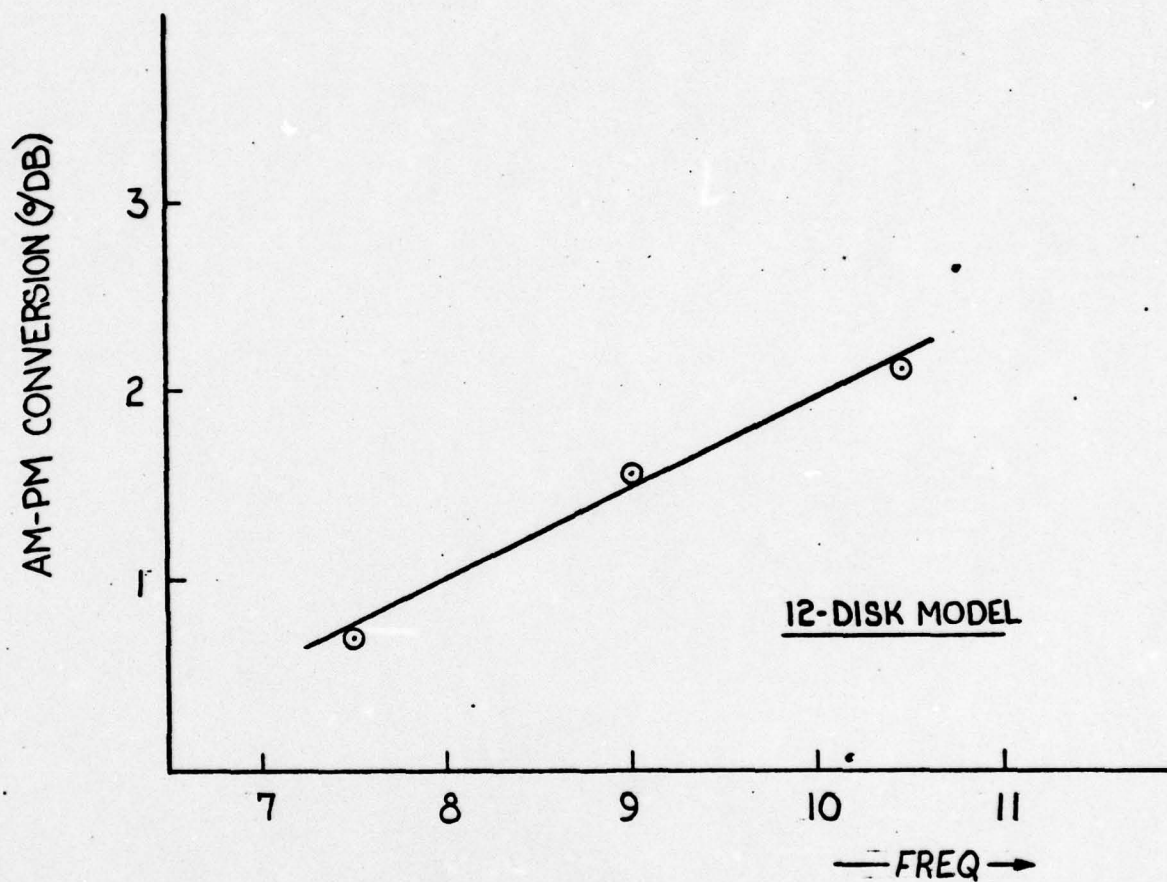


FIG. 14 OPTIMUM AM-PM CONVERSION VS. FREQUENCY



The values of synchronism parameter  $b$  at which the minimum AM-PM occur are plotted in Figure 15. This data indicates that the optimum circuit is one having a constant undervoltaged characteristic with  $X_j \approx .6$ . The tube circuit is undervoltaged over the entire frequency band and is increasingly more undervoltaged at the lower frequency end of the band. In Figure 16, the lossy-line tube design for the output power section is shown for 33 kV and 6A. Note that locus is very close to the optimum condition from about 7.2 GHz to about 9.7 GHz. The circuit dispersion diagram is shown in Figure 17. The line labeled  $u_0$  represents the velocity of the electron beam. Higher values of cathode voltage would be represented by lines of greater slope such that they would intersect the circuit dispersion characteristics. Note that the circuit velocity is always higher than the beam velocity or the circuit is undervoltaged. Note too that the undervolting is less at the high frequency end than at the low frequency end. This is precisely the dispersion characteristic required to produce the optimum AM-PM demonstrated over the full bandwidth at a single value of cathode voltage.

## 2.2 The Space Charge Parameter - QC

The space charge parameter is a measure of beam perveance and circuit quality. Low values of QC occur for low perveance and high circuit interaction impedance.

It seems plausible that low QC is advantageous to AM-PM since if the circuit forces are relatively much stronger than the space charge forces then nonlinear effects are minimized. The phase distortion and harmonic generation must also be decreased since they are nonlinear processes.

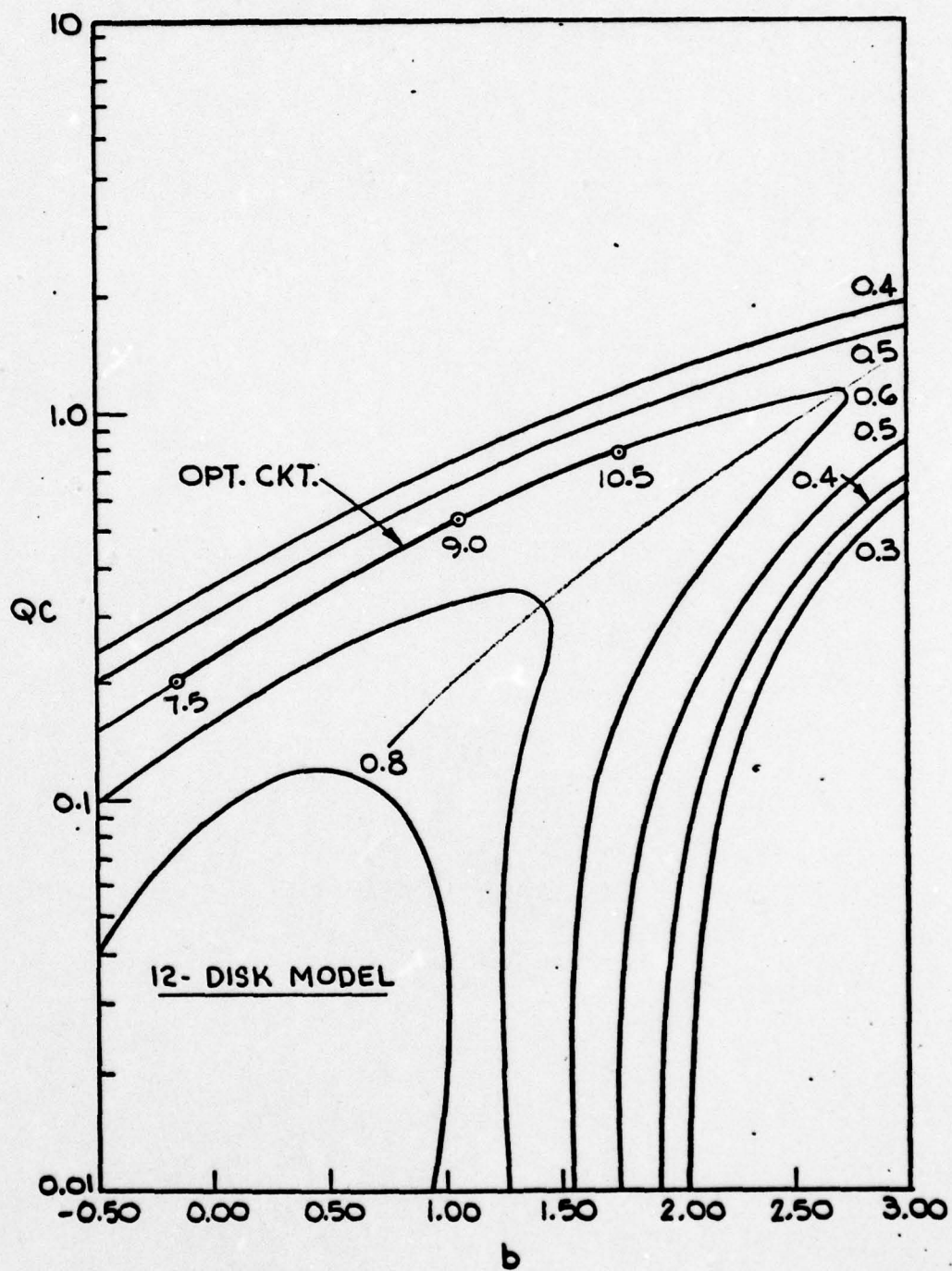


FIG. 15 GAIN CHARACTERISTICS FOR OPTIMUM CIRCUIT

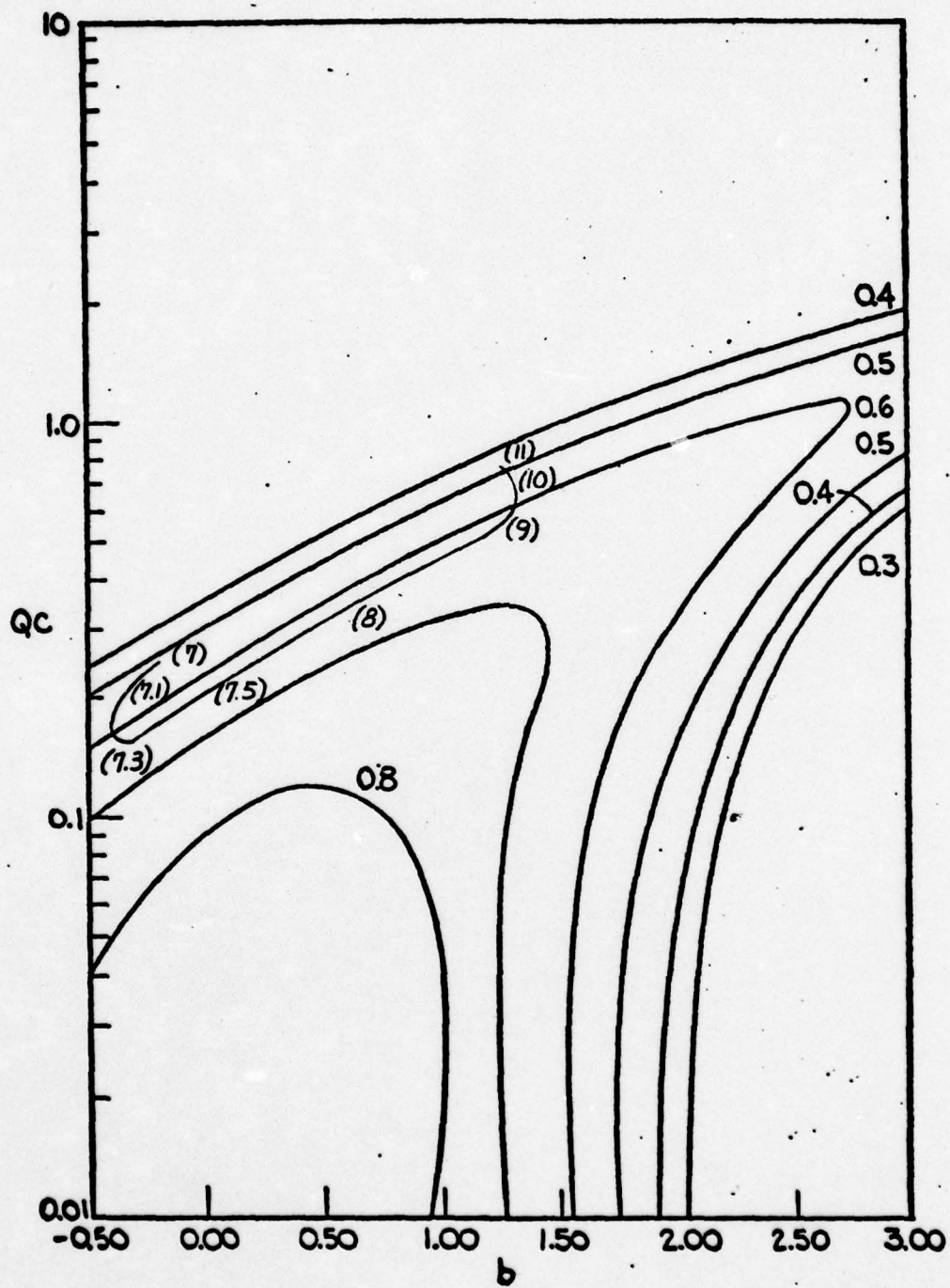


FIG.16 GAIN CHARACTERISTICS FOR L5631, S/N 2001.



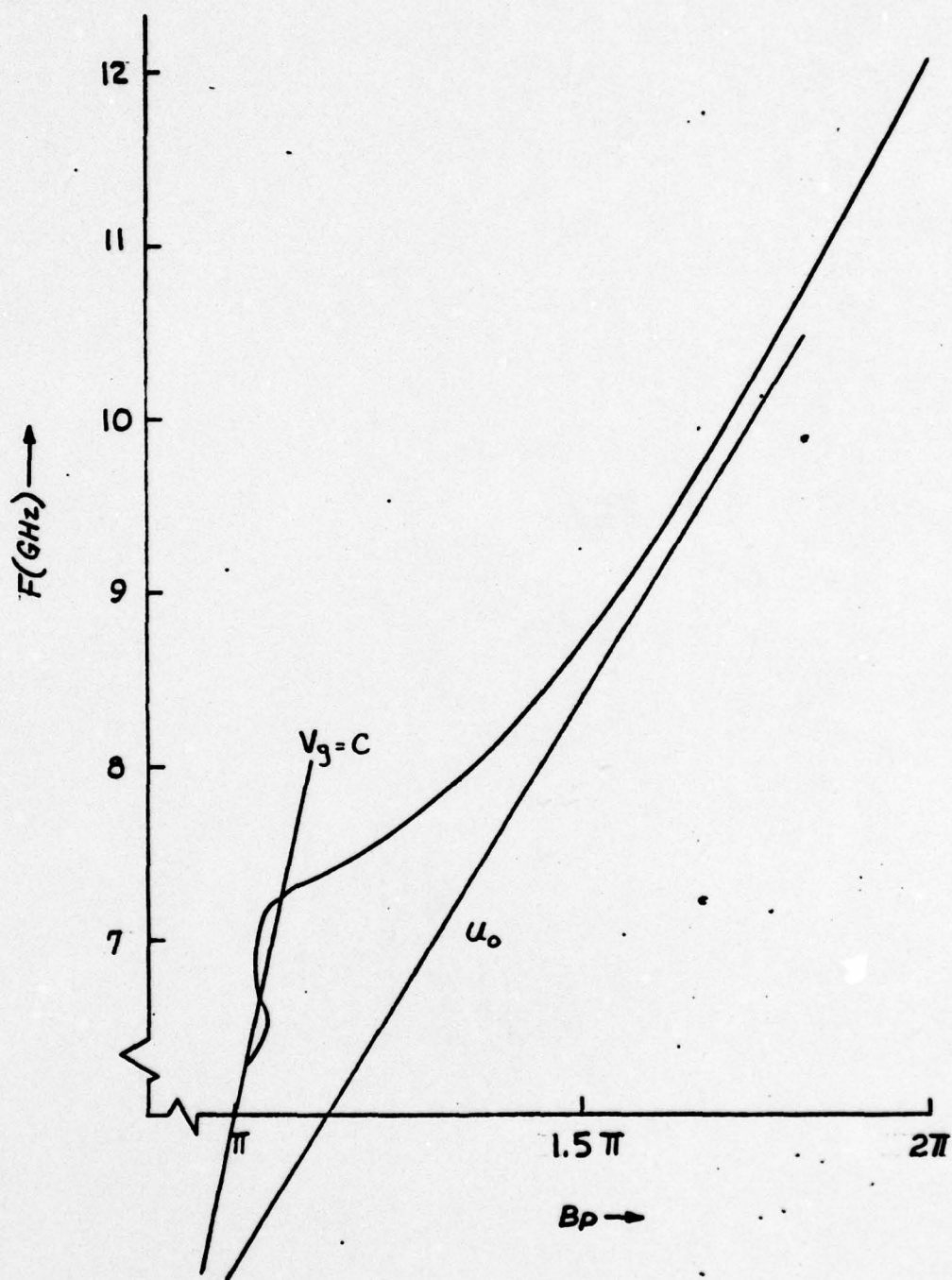


FIG. 17 L-5631, S/N 2001  
DISPERSION CHARACTERISTICS  
(UNLOADED CIRCUIT)

In Figure 18 curves from J. R. Pierce's "Traveling-Wave Tubes" are shown which show how the gain locus varies as a function of QC. For high values of QC the gain falls off more rapidly with b than for low values of QC. Thus b may be decreased by a larger percentage at low QC before the gain begins to decrease rapidly. Lower values of  $\eta/G\lambda$  are obtained than at higher QC. The efficiency is higher at lower QC so that a nearly constant power condition is reached even though  $b_0 - b_{opt}$  is higher at low QC.

It is also more apparent now that the lowest distortion tube is also the one capable of the highest efficiency if it were run in an overvoltaged condition. The parameter C should be maximum. This ensures QC is low since  $QC \propto 1/C^2$ .

### 2.3 The Loss Parameter - d:

The loss parameter d is a measure of the circuit loss. The loss per cavity has a very important influence on the AM-PM conversion in a TWT. Figure 19 is included here to show how loss affects the AM-PM conversion in the loss line tube. This computer analysis was done at 7.5 GHz with  $b = 0$ . Therefore b, QC and C are all near optimum. AM-PM conversion is plotted as a function for  $P_0$  (dBm) for various values of d, the loss parameter. For  $d = .2$  which is near the correct value for the loss line tube, the output power is about 72 dBm and AM-PM is about  $1^\circ/\text{dB}$ . Doubling the circuit loss,  $d = .4$ , results in nearly double the AM-PM conversion at saturation. The saturated power has also been degraded by about 4 dB.

Loss should never be introduced intentionally into the output power section which is the length of the tube back from the output having about 20 dB small signal gain. However, the circuit

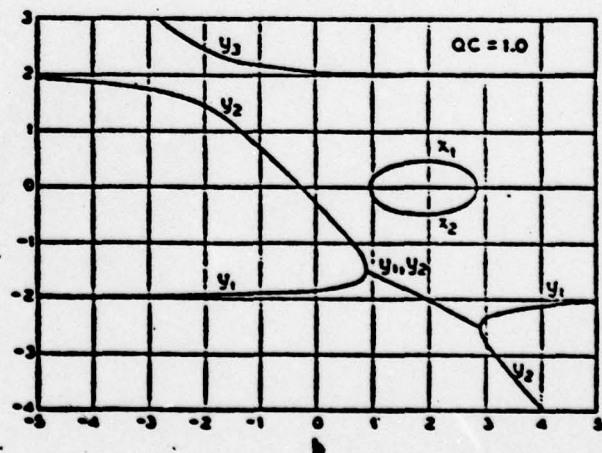
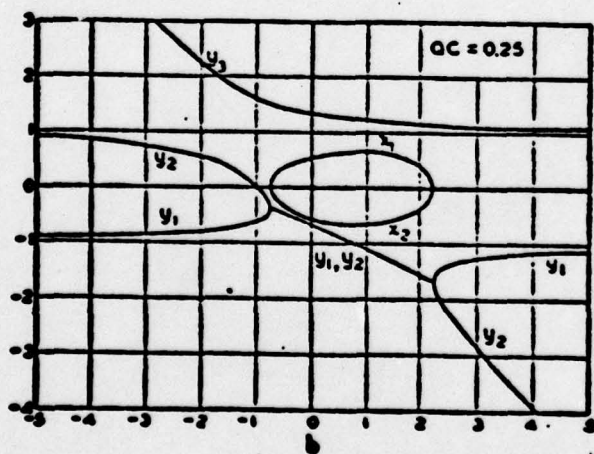
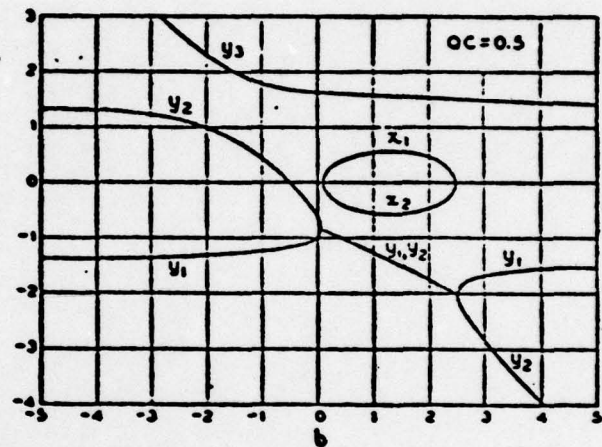
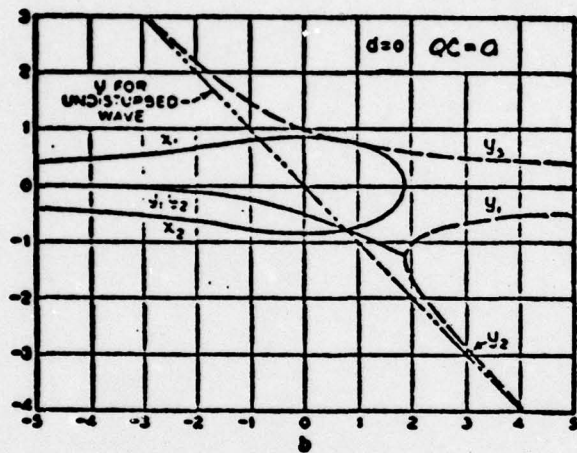


FIG. 18 GAIN CHARACTERISTICS FOR VARIABLE SPACE CHARGE PARAMETER.



$QC = .192$   
 $C = .12$   
 $F = 7.5 \text{ GHz}$   
 $b = 0$

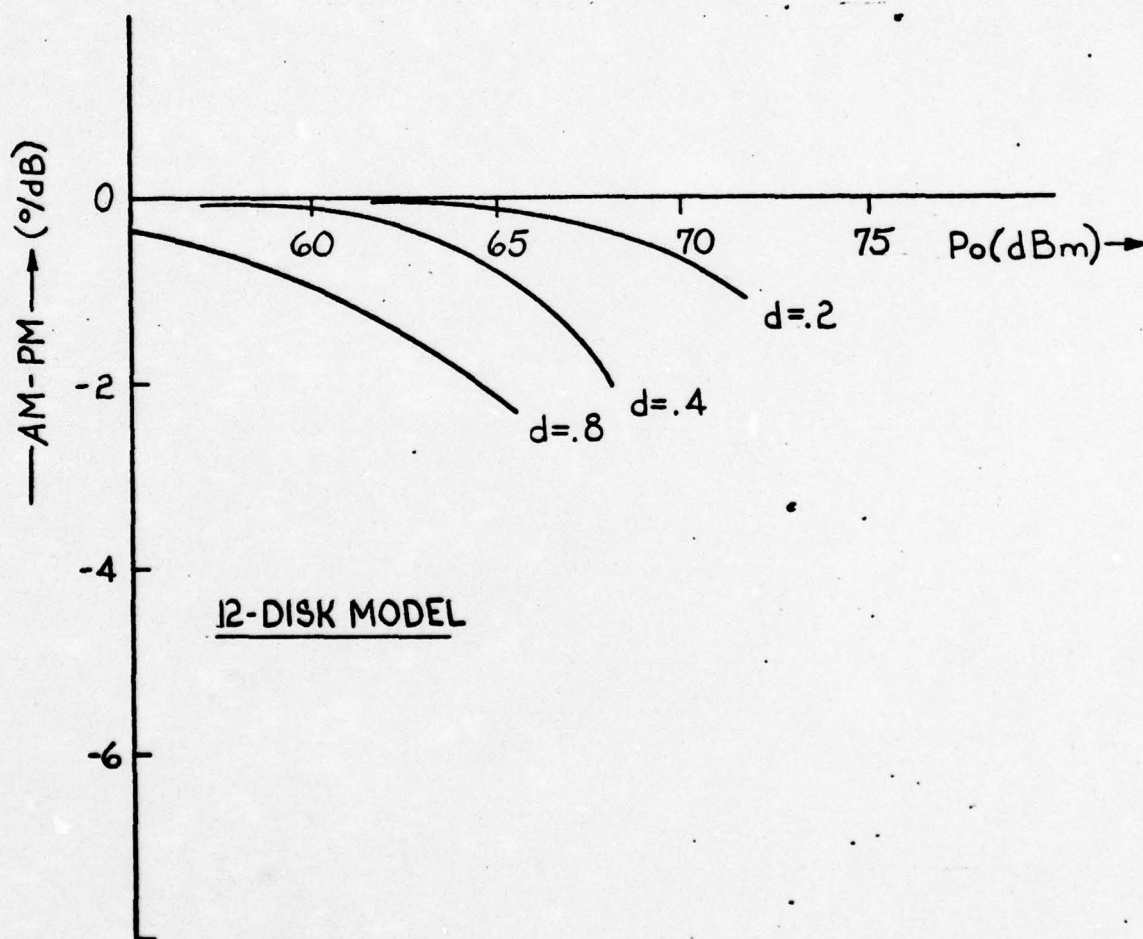


FIG. 19 AM-PM CONVERSION VS. POWER OUTPUT LOSS PARAMETER VARIABLE.

itself has intrinsic loss due to skin effect losses and this cannot be avoided. In PPM focused coupled cavity tubes where iron pole pieces are used to convey the magnetic flux from the magnets to the interaction area, the iron pole pieces should be copper plated to reduce this resistivity to as low a value as possible. Solenoid tube circuits which are fabricated from bulk OFHC copper have the lowest intrinsic resistivity possible.

The dependence of AM-PM on circuit loss has been treated by both Ober<sup>11</sup> and Nishihara<sup>17</sup>. Ober contends that the circuit loss is detrimental because it limits the degree of saturation, the beam modulation and the negative phase generation. By moving the attenuator section toward the input of the tube, Ober has demonstrated significant AM-PM improvement. Nishihara made similar measurements, and concluded that the "phase deviation increases exponentially .... when the length of the output section decreases or when the attenuator is shifted towards the output side ....; it is found that the effect of the attenuator is negligible when the small signal gain of the output section is more than about 25 dB".

### 3.0 DEVELOPMENT OF DESIGNS WHICH COULD SATISFY THE DESIRED SPECIFICATION

During this study, several designs were studied which could possibly satisfy the requirements of the contract. Two specific broadband designs received considerable attention during this study:

1. A button stabilized tube scaled from our L-5388 and L-5511 designs.
2. A loss line stabilized tube scaled from our L-5631, S/N 2001 design.

These designs are discussed in detail in Sections 3.1 and 3.2 respectively.

Narrow band designs, i.e. designs having cold bandwidths approximating the hot bandwidth requirement were eliminated primarily because our computer results and laboratory measurements show the AM-PM requirement cannot be met over the high frequency portion of the band with a saturated tube. We did consider operating narrow band tubes in the small signal region, but limitations were placed on the tube slow-wave circuit. In addition, large output power variation with frequency would be expected in a non-saturated situation.

#### 3.1 Design I -- Wideband Circuit, Loss-Button Stabilized

The circuit would be scaled from our present wideband button stabilized family of tubes. Figures 20 and 21 show the power output and AM-PM characteristics from representative samples of these tubes. The specified band is shown scaled to an appropriate frequency region over which the power output and AM-PM requirements are met. Note that the band is oriented near the lower band edge of hot tube bandwidth. It has been shown in Section 2 that the best AM-PM characteristics are found at the low frequency end



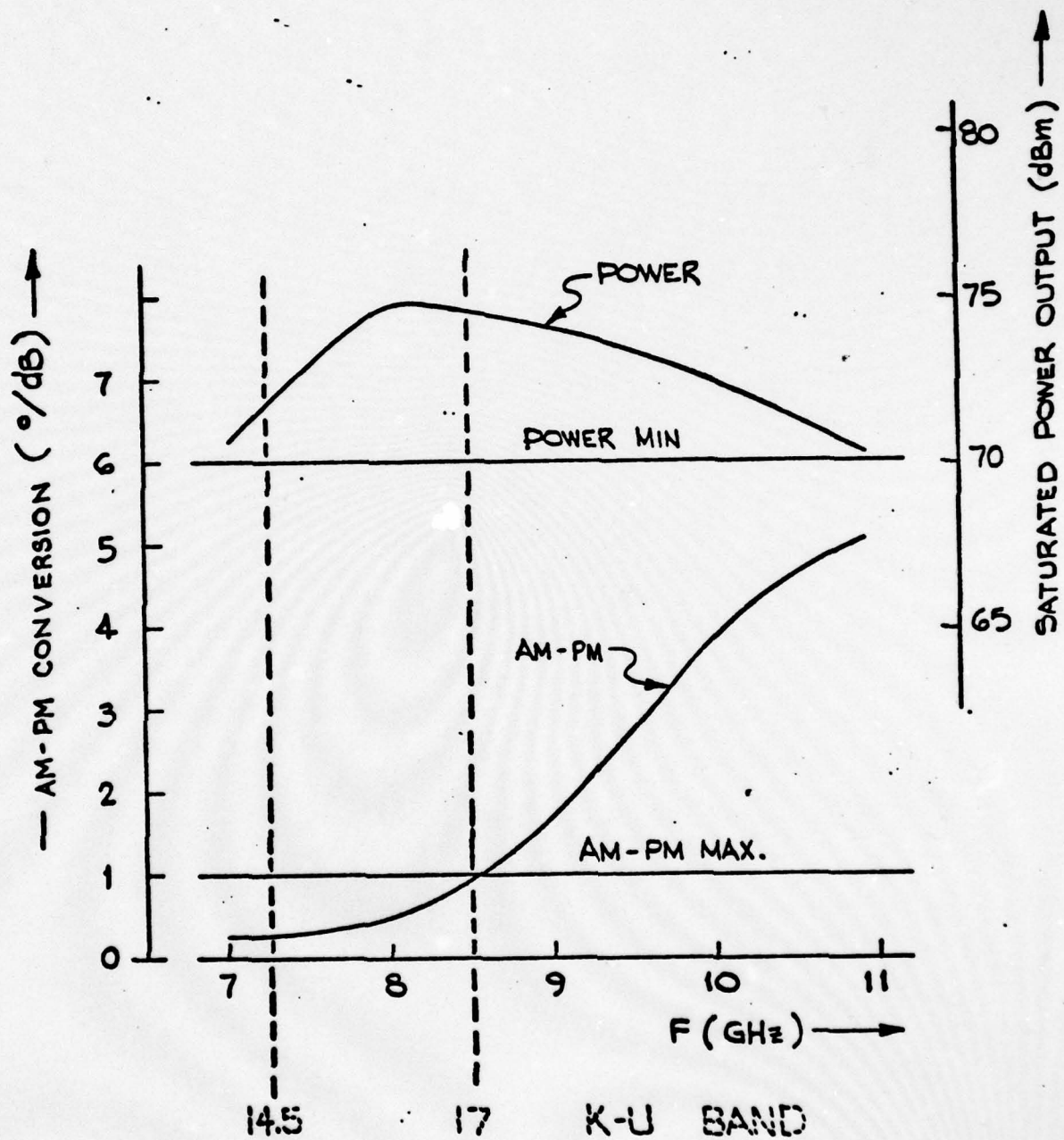


FIG.20 L-5388 S/N 2015  
 AM - PM VS FREQUENCY  
 SAT. POWER VS FREQUENCY

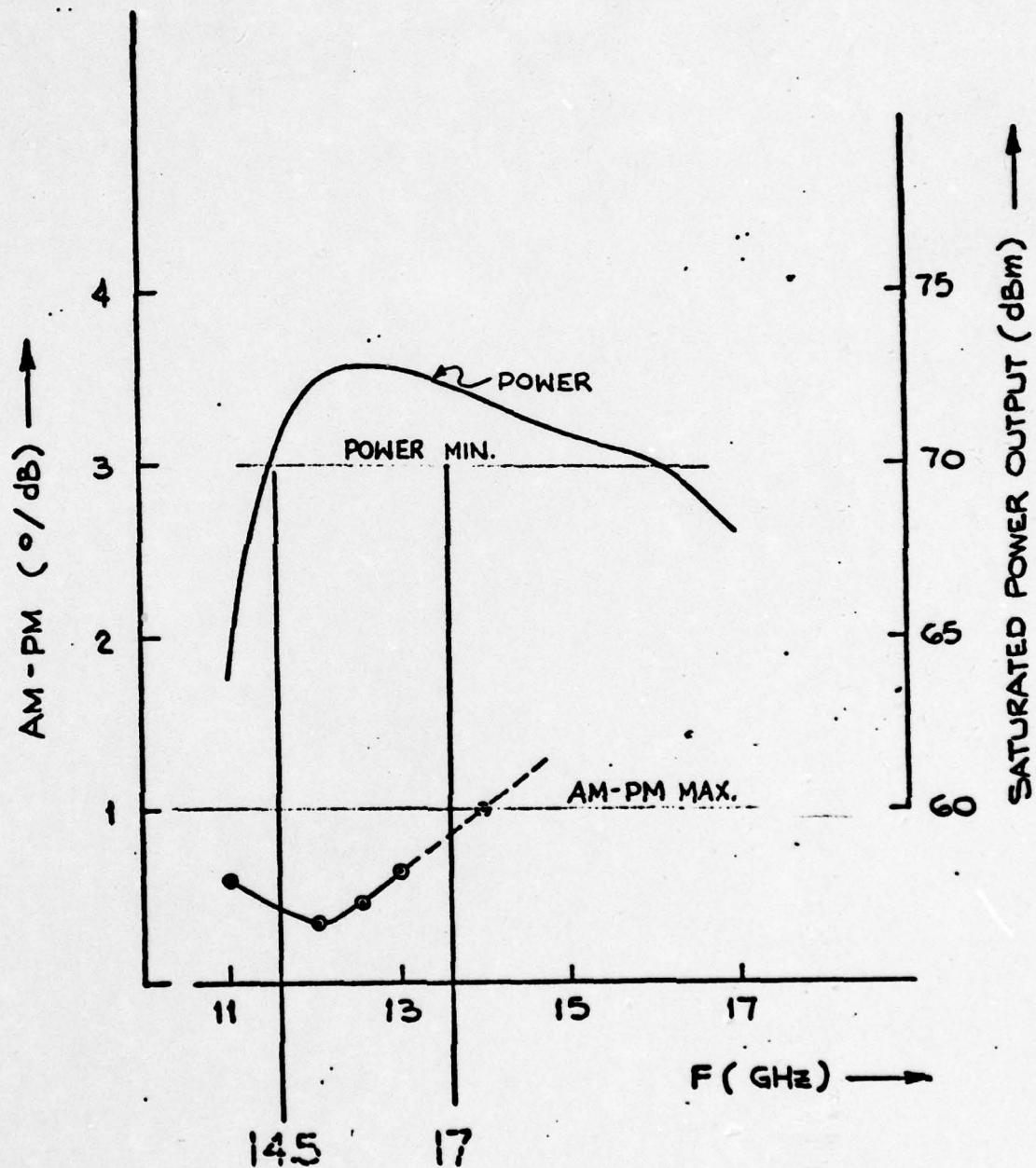


FIG. 21 L-5511 9/N 2007  
 AM-PM VS FREQUENCY  
 SAT. POWER VS FREQUENCY

of the band. The proper scaling then leads to a hot tube bandwidth of 14 - 22 GHz for this tube. The scale factor from the present L-5511 Ku-Band tube is .785:1.

The preliminary mechanical design for the tube is shown in Figure 22. We have chosen solenoid focusing for the following reasons:

1. High duty - The specified 4% level could be achieved with PPM focusing but the design would be close to the thermal limit. By choosing a solenoid design an 8% level could be easily obtained. Since the long term objective is in this 8% neighborhood, it is advisable to adopt the solenoid design now.
2. Efficiency - Although focusing is related to duty factor, it is also important to efficiency since electrons collected on the circuit cannot contribute to the amplification and power processes.
3. AM-PM - The loss per cavity has a very important influence on the AM-PM conversion in a TWT as has been shown in Section 2.0. An all OFHC copper circuit will provide the minimum possible circuit losses.

The solenoid design shown in Figure 22 is similar to the design used for a high-power Ku-Band production tube. The length has been increased to accommodate the circuit length required. The coils are shown wound on the circuit. There are five coils in the center portion of the solenoid and two larger ones near the ends. These coils are wound on the tube after exhaust. They are composed of many wraps of thin copper tapes separated electrically with thin mylar tape.

The coils may be interconnected in series or parallel depending upon the final watt-ampere characteristic required. The return path (shown dotted) is placed completing the magnetic circuit. The solenoid is cooled in series with the tube. As shown in the



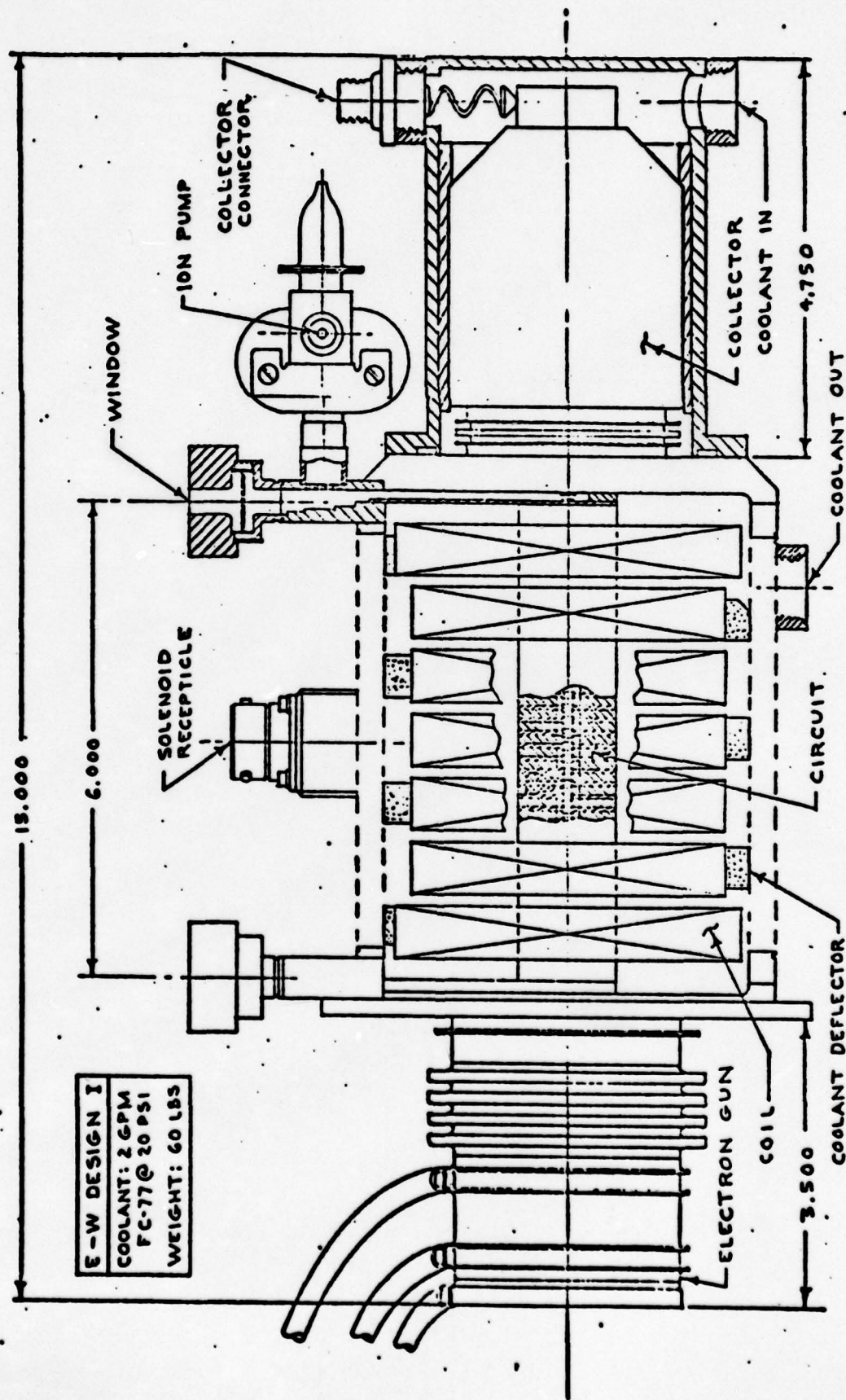


FIG. 22 E-W TUBE - DESIGN I

drawing the coolant enters the collector of the tube, goes through the tube circuit to the gun pole piece and then flows through the solenoid from input to output. Coolant deflectors are used in the solenoid to force the coolant to travel in a zig-zag path around the coils. The coolant output is shown near the output end of the tube.

The solenoid field was determined to be a nominal 2500 gauss. The field will be tapered near the input and output to obtain the optimum characteristics in hot test. The end coils are separately accessible for this purpose.

The predicted transmission without RF from the computer runs is 99.5%. (See Figure 23.) No runs have been made, as yet, with the 3-dimensional program. However, similar tubes have been run with RF and shown to have nearly 100% transmission with the correct output taper. *meaningless computation*

The same gun used in the present Navy J-Band tube, the L-5511, will be used on this tube. Because the beam tunnel is now *- Effect on focusing* smaller, the gun placement and magnetic field had to be determined.

Dr. J. R. Hechtel and his staff made several computer runs. The chosen design parameters are summarized in Table 1.

The L-5511 window cannot be used on this tube because it has been designed for the 11 - 17 GHz band. The match above 17 GHz deteriorates rapidly. The window must be redesigned to operate over the 14 - 22 GHz band. A good match to 20 GHz should be sufficient since we plan to put considerable loss above this frequency. The redesign should be straight-forward since the wide bandwidth has already been achieved over lower frequency bands.

Preliminary computer runs were made to determine gain, power and AM-PM conversion for the scaled tube. The circuit parameters used

$V_0 = 33K$	$B_0 = 2500$
$\mu P = 0.8$	$B_K = 0$
$I_0 = 4.8A$	GUN = L-5511

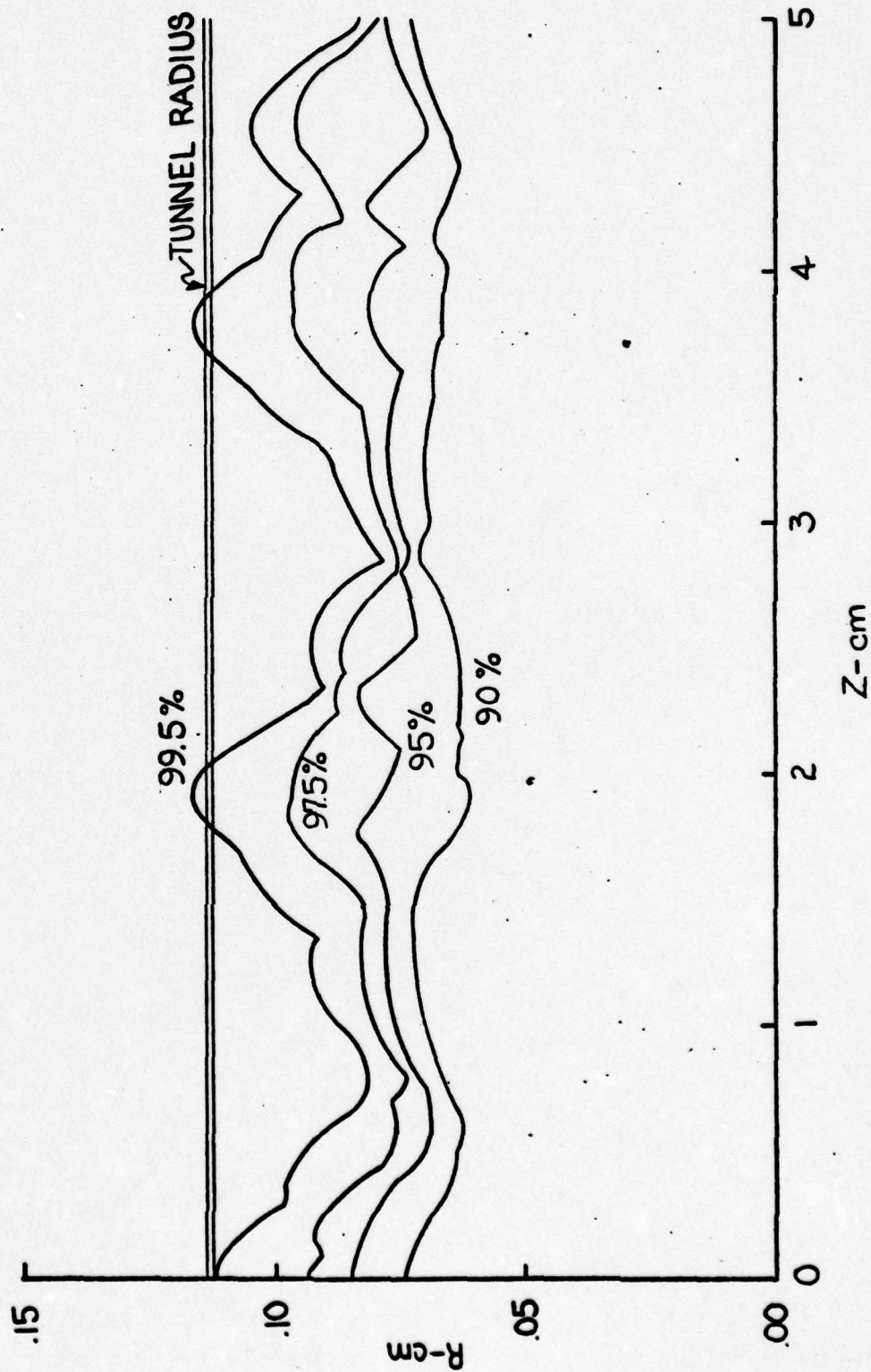


FIG. 23 TRANSMISSION CHARACTERISTICS FOR E-W TUBE.



TABLE 1

Gun Type	L-5511
Cathode Diameter	.400 in.
Cathode Half Angle	30°
Cathode-Anode Spacing	.300 in.
Heater Voltage	11 V
Heater Current	3 amps
Cathode Voltage	32 kV
Microperveance	.8 micropervs
Cathode Current	5 amps
Control Grid Voltage	365V
Focusing Field	2500 gauss
Predicted Beam Transmission (w/o RF)	99.5%

Chosen Design Parameters

were the same as determined for lossy-line circuit except for circuit loss parameters. Cold test parts were built to determine the attenuation as a function of frequency across the frequency band. The cold test parts were made out of OFHC copper since this is what would be used in a solenoid focused tube.

The results of a typical computer run at 15 GHz are shown in Tables 2 and 3. The output power at saturation was about 16 kW. The large signal gain was 63 dB and the AM-PM conversion for  $\pm 3$  dB around saturation was less than  $1^\circ/\text{dB}$ .

At 16 GHz the computer results are shown in Tables 4 and 5. The saturated power was 24 kW, the large signal gain was 44 dB and the AM-PM conversion was about  $1^\circ/\text{dB}$  around saturation.

At 17 GHz the computer results are shown in Tables 6 and 7. The output power at saturation was 27 kW and the large signal gain was 42 dB. The AM-PM conversion for  $\pm 3$  dB around saturation was about  $1^\circ/\text{dB}$ .

### 3.2 Design II -- Wideband Circuit, Lossy-Line Stabilized

The circuit for this design would be scaled from the I-Band lossy-line tube, the L-5631, S/N 2001. The hot bandwidth would be 12.0 - 18.9 GHz. The frequency of 12.0 GHz corresponds to 7.0 GHz and 18.9 GHz corresponds to 11.0 GHz. This scale factor is .585:1.

Figure 24 shows the saturated output power and AM-PM data from the L-5631, S/N 2001. Superimposed on this data are the projected Ku-Band scaled frequencies. The purpose of this figure is to show the relative orientation of the objective band with relation to the full hot band of the tube. Note that the 14.5 - 17 objective band has been oriented nearer the high end of the hot band than

PROGRAM VAI18A

RUN TYPE: TIMESHARING (TMS) OR REMOTE JOB (RJE) ? TMS  
 INPUT DATA ON FILE (Y/N) ? N  
 CASE IDENTIFICATION ? 15GHZ  
 BEAM KV. MU P ? 32,.873  
 BEAM CURRENT 4.9973 AMP  
 TUNNEL DIA (INCH), B/A ? .092,.6  
 FREQUENCY (GHZ) ? 15  
 TOTAL NO. OF CAVITIES (INCL. SEVER CAVITIES) ? 38  
 ANY TAPERS OR STEPS (OTHER THAN SEVERS) (Y/N) ? N  
 FOR CAVITY #1 AND EACH BREAK POINT ENTER PHASE VEL.(M/S/IE7)  
 OR ENTER 'S' IF SAME AS LAST ONE IN ALL PARAMETERS  
 AFTER 2ND ? ENTER IMPEDANCE, LOSS(DB/CAV), CAV PERIOD(INCH), GAP(INCH)  
 BREAKPOINT NO. 1, CAVITY NO. 1 ? 10.05  
 ? 40,.28,.157,.048  
 NUMBER OF SEVER CAVITIES (MAX. 6) ? 2  
 ENTER SEQUENCE NUMBERS ? 16,17  
 CHANGES (Y/N) ? N  
 FILE DATA (Y/N) ? N

MEAN POT. DEP -716.91 VOLTS, BEAM VEL. 9.9972E+07 M/S  
 LAMBDA E = 6.66 MM; BETA E = 942.7  
 DISK CHARGE 1.3882E-11 CB  
 PLASMA KVLGTH 26.94 MM; PLASMA FREQ 2.44454E+10 R/S  
 REDUCED PLASMA FREQ 1.04658E+10 R/S  
 POT. DEP. FROM SUM OF DISKS -719.08 VOLTS  
 VOLTS AT NODES 0 THRU 12 DUE TO DISC AT NODE 0:  
 -185.346 -118.214 -65.178 -36.454 -20.503 -11.559 -6.526  
 -3.642 -2.099 -1.211 -.729 -.493 -.422  
 FIRST SECTION VALUES:  
 BETA(-1)= 937.8, GAMMA(-1)= 883.5, GAMMA\*A=1.0323  
 M1 = .9464, M2 = .8035  
 TOTAL IMPEDANCE 967 OHMS  
 PIERCE'S C = .11602, SMALL B = -.045  
 QC = .18553, SMALL D = .074  
 ASYMPTOTIC GAIN 3.26 DB/CAVITY  
 PEAK GAIN 3.93 AT ABOUT CAVITY 6  
 PHASE SHIFT PER CAVITY = 214.3 DEG ( 1.190PI)  
 VOLTAGE ATTENUATION FACTOR PER CAV.= .9683  
 U1= 404.49, U3= 106.34, U5= 12.84

TABLE 2  
 VAI18A- 15 GHz



OLD. VAI118B  
\*RDY-SBA\*  
KHE.M=6192  
VAI118B: TWT BEAM WITH ABSOLUTE PHASE OUTPUT

08/10/78.

CASE: 15  
USE 12 OR 24 DISC MODEL ? 12  
DRIVE POWER, WATTS ? .008

PIN= .8E-02 WATTS  
FIRST PASS (Y/N) ? Y

CAV. NO.	VOLTS R-F	POWER WATTS	GAIN DB	I-FUND /I-DC	I-2ND /I-DC	I-3RD /I-DC	ABS PHASE	REL PHASE	CAV. LOSS WATTS	EFFIC. PCNT.	EN. BAL. PCNT.
1	3.93	.008	.00	.0000	.0000	.0000	.0	180.0	.000	.00	100.00
3	3.73	.007	-.46	.0005	.0002	.0001	342.5	191.1	.000	-.00	100.00
5	5.66	.017	3.19	.0014	.0004	.0002	297.3	230.8	.001	.00	100.00
7	11.20	.065	9.09	.0023	.0006	.0005	267.1	243.0	.004	.00	100.00
9	18.43	.175	13.41	.0035	.0016	.0015	240.4	233.3	.011	.00	99.99
11	24.45	.448	17.48	.0062	.0027	.0025	207.5	231.1	.028	.00	99.99
13	50.92	1.340	22.24	.0107	.0048	.0048	174.3	235.5	.084	.00	99.99
15	67.40	3.948	26.93	.0180	.0087	.0084	142.4	235.1	.247	.00	99.99
17	3.93	.008	.00	.0272	.0124	.0123	79.4	268.6	.000	.00	99.94
19	101.01	5.274	28.19	.0287	.0136	.0206	60.7	262.7	.329	.00	99.96
21	160.26	13.278	32.20	.0278	.0281	.0297	38.5	227.8	.829	.01	99.98
23	239.40	29.621	35.69	.0587	.0386	.0204	357.6	226.0	1.849	.02	100.00
25	465.23	111.860	41.46	.1081	.0497	.0383	319.5	238.7	6.984	.07	99.95
27	612.24	340.967	46.30	.1567	.0944	.0601	290.9	236.5	21.289	.21	99.94
29	1250.20	807.803	50.04	.2463	.1322	.1325	260.2	228.4	50.438	.51	99.79
31	1999.52	2066.305	54.12	.4456	.1503	.1958	223.7	229.4	129.016	1.29	99.67
33	3260.91	5563.296	58.42	.7157	.3595	.2653	186.9	229.9	347.361	3.48	99.68
35	4721.69	11522.272	61.59	.9972	.4690	.3907	150.7	218.7	719.428	7.21	97.80
37	5012.53	12985.482	62.10	.9912	.1345	.6758	112.8	186.7	810.787	8.12	94.27
39	5476.48	15500.530	62.87	.8575	.3697	.6641	98.7	213.0	967.822	9.69	94.38

T = 1.51667E-09 SEC, NO = 273 STEPS  
TOTAL CAVITY LOSSES = 4812.880 W  
TOTAL SEVER POWER = 4.0 W  
ELECTRONIC EFFIC. = 12.71 PCI  
RESIDUAL BEAM K.E. = 81.68 PCI.

TABLE 3. VAI118B - 15 GHz

RUN TYPE: TIMESHARING (TMS) OR REMOTE JOB (RJE) ? TMS  
 INPUT DATA ON FILE (Y/N) ? N  
 CASE IDENTIFICATION ? 16  
 BEAM KV, MU P ? 32..873  
 BEAM CURRENT 4.9973 AMP  
 TUNNEL DIA (INCH), B/A ? .092..6  
 FREQUENCY (GHZ) ? 16  
 TOTAL NO. OF CAVITIES (INCL. SEVER CAVITIES) ? 38  
 ANY TAPERS OR STEPS (OTHER THAN SEVERS) (Y/N) ? N  
 FOR CAVITY #1 AND EACH BREAK POINT ENTER PHASE VEL.(M/S/1E7)  
 OR ENTER 'S' IF SAME AS LAST ONE IN ALL PARAMETERS  
 AFTER 2ND ? ENTER IMPEDANCE, LOSS(DB/CAV), CAV PERIOD(INCH), GAP(INCH)  
 BREAKPOINT NO. 1, CAVITY NO. 1 ? 9.57  
 ? 16..21..157..048  
 NUMBER OF SEVER CAVITIES (MAX. 6) ? 2  
 ENTER SEQUENCE NUMBERS ? 16,17  
 CHANGES (Y/N) ? N  
 FILE DATA (Y/N) ? N

MEAN POT. DEP -716.91 VOLTS, BEAM VEL. 9.9972E+07 M/S  
 LAMBDA E = 6.25 MM; BETA E = 1005.6  
 DISK CHARGE 1.3014E-11 CB  
 PLASMA W.LGTH 26.94 MM; PLASMA FREQ 2.44454E+10 R/S  
 REDUCED PLASMA FREQ 1.10356E+10 R/S  
 POT. DEP. FROM SUM OF DISKS -719.08 VOLTS  
 VOLTS AT NODES 0 THRU 12 DUE TO DISC AT NODE 0:  
 -175.376 -114.889 -65.638 -38.023 -22.154 -12.942 -7.574  
 -4.444 -2.623 -1.575 -.990 -.696 -.607  
 FIRST SECTION VALUES:  
 BETA(-1)= 1050.5, GAMMA(-1)= 995.5, GAMMA\*A=1.1632  
 M1 = .9330, M2 = .7610  
 TOTAL IMPEDANCE 557 OHMS  
 PIERCE'S C = .08548, SMALL B = .522  
 QC = .33473, SMALL D = .068  
 PHASE SHIFT PER CAVITY = 240.0 DEG ( 1.333PI)  
 VOLTAGE ATTENUATION FACTOR PER CAV.= .9761  
 U1= 404.49, U3= 106.34, U5= 12.84

TABLE 4  
 VAI18A - 16 GHz



# PROGRAM VAI18B

VAI18B: TWT BEAM WITH ABSOLUTE PHASE OUTPUT 08/10/78.

CASE: 16  
USE 12 OR 24 DISC MODEL ? 12  
DRIVE POWER, WATTS ? 1

PIR= 1 WATTS  
FIRST PASS (Y/N) ? Y

CAV. NO.	VOLTS R-F	POWER WATTS	GAIN DB	I-FUND /I-DC	I-2ND /I-DC	I-3RD /I-DC	ABS PHASE	REL PHASE	CAV. LOSS WATTS	EFFIC. PCNT.	EN. BAL. PCNT.
1	33.37	1.000	.00	.0000	.0000	.0000	.0	180.0	.047	.00	100.00
3	33.14	.986	-.06	.0041	.0019	.0005	350.6	201.2	.047	-.00	99.98
5	44.43	1.772	2.49	.0113	.0037	.0019	329.4	234.8	.084	.00	99.99
7	70.97	4.522	6.55	.0182	.0061	.0061	314.5	249.0	.213	.00	100.00
9	104.59	9.820	9.92	.0240	.0134	.0113	302.6	244.8	.464	.01	100.01
11	150.98	20.465	13.11	.0376	.0191	.0152	286.7	240.4	.966	.01	99.99
13	229.92	47.461	16.76	.0614	.0304	.0241	269.3	241.9	2.240	.03	99.99
15	347.90	109.719	20.41	.0897	.0484	.0362	253.6	242.9	5.189	.07	99.91
17	33.37	1.000	.00	.1261	.0664	.0654	216.5	267.2	.047	.00	99.83
19	275.14	67.964	18.32	.1253	.0704	.0682	208.4	266.1	3.208	.04	99.80
21	433.19	168.476	22.27	.1063	.1069	.1357	196.8	239.3	7.953	.10	99.78
23	607.40	331.231	25.20	.1874	.1481	.0826	173.3	229.2	15.635	.21	99.88
25	999.43	896.770	29.53	.3013	.1935	.1338	150.2	242.5	42.331	.56	100.01
27	1534.10	2112.936	33.25	.3995	.2412	.1987	133.0	240.0	99.739	1.32	99.95
29	2110.69	3999.701	36.02	.5418	.3838	.2599	113.8	229.1	188.801	2.50	99.51
31	2789.81	6987.569	38.44	.7487	.4895	.4969	90.3	223.7	329.840	4.37	98.96
33	3408.06	10427.901	40.18	.8438	.5946	.6186	66.8	224.0	492.237	6.52	97.84
35	4135.04	15351.003	41.86	.7706	.3456	.3101	49.4	223.2	724.626	9.60	97.75
37	4846.69	21089.630	43.24	.7682	.2871	.3010	35.4	223.8	995.511	13.19	96.84
38	5146.17	23794.881	43.77	.8112	.0987	.2666	28.7	219.0	1123.210	14.88	95.69

T = 1.51562E-09 SEC, NO = 291 STEPS  
TOTAL CAVITY LOSSES = 6382.621 W  
TOTAL SEVER POWER = 110.9 W  
ELECTRONIC EFFIC. = 18.94 PCT  
RESIDUAL BEAM K.E. = 76.75 PCT.

TABLE 5 VAI18B - 16GHz



# PROGRAM VAI18A

RUN TYPE: TIMESHARING (TMS) OR REMOTE JOB (RJE) ? TMS  
 INPUT DATA ON FILE (Y/N) ? N  
 CASE IDENTIFICATION ? UPPER F  
 BEAM KV, MU P ? 32,.873  
 BEAM CURRENT 4.9973 AMP  
 TUNNEL DIA (INCH), B/A ? .092,.6  
 FREQUENCY (GHZ) ? 17  
 TOTAL NO. OF CAVITIES (INCL. SEVER CAVITIES) ? 38  
 ANY TAPERS OR STEPS (OTHER THAN SEVERS) (Y/N) ? N  
 FOR CAVITY #1 AND EACH BREAK POINT ENTER PHASE VEL.(M/S/1E7)  
 OR ENTER 'S' IF SAME AS LAST ONE IN ALL PARAMETERS  
 AFTER 2ND ? ENTER IMPEDANCE, LOSS(DB/CAV), CAV PERIOD(INCH), GAP(INCH)  
 BREAKPOINT NO. 1, CAVITY NO. 1 ? 9.38  
 ? 12,.15,.157,.048  
 NUMBER OF SEVER CAVITIES (MAX. 6) ? 2  
 ENTER SEQUENCE NUMBERS ? 16,17  
 CHANGES (Y/N) ? N  
 FILE DATA (Y/N) ? N

MEAN POT. DEP -716.91 VOLTS, BEAM VEL. 9.9972E+07 M/S  
 LAMEDA E = 5.88 MM; BETA E = 1068.4  
 DISK CHARGE 1.2248E-11 CB  
 PLASMA KVLOTH 26.94 MM; PLASMA FREQ 2.44454E+10 R/S  
 REDUCED PLASMA FREQ 1.15858E+10 R/S  
 POT. DEP. FROM SUM OF DISKS. -719.08 VOLTS  
 VOLTS AT NODES 0 THRU 12 DUE TO DISC AT NODE 0:  
 -166.417 -111.642 -65.823 -39.330 -23.641 -14.252 -8.610  
 -5.218 -3.185 -1.982 -1.293 -.941 -.832  
 FIRST SECTION VALUES:  
 BETA(-1)= 1138.7, GAMMA(-1)= 1081.6, GAMMA\*A=1.2637  
 M1 = .9216, M2 = .7277  
 TOTAL IMPEDANCE 550 OHMS  
 PIERCE'S C = .07767, SMALL B = .847  
 QC = .39684, SMALL D = .049  
 PHASE SHIFT PER CAVITY = 260.2 DEG ( 1.445PI)  
 VOLTAGE ATTENUATION FACTOR PER CAV.= .9829  
 U1= 404.49, U3= 106.34, U5= 12.84

## TABLE 6

VAI18A - 17 GHz

CASE: UPPER F  
USE 12 OR 24 DISC MODEL ? 12  
DRIVE POWER, WATTS ? 1.5

PII= 1.5 WATTS  
FIRST PASS (Y/N) ? Y

CAV. NO.	VOLTS P-F	POWER WATTS	GAIN DB	I-FUND /I-DC	I-2ND /I-DC	I-3RD /I-DC	ABS PHASE	REL PHASE	CAV. LOSS WATTS	EFFIC. PCNT.	EN. BAL. PCNT.
1	40.63	1.500	.00	.0000	.0000	.0000	.0	180.0	.051	.00	100.00
3	41.64	1.576	.21	.0050	.0023	.0006	351.3	209.6	.053	.00	99.98
5	58.01	3.058	3.09	.0139	.0047	.0024	335.7	244.1	.104	.00	99.99
7	80.87	7.176	6.80	.0203	.0083	.0076	327.7	256.8	.244	.00	100.02
9	127.76	14.832	9.95	.0277	.0177	.0133	320.0	251.1	.504	.01	100.03
11	189.05	32.476	13.35	.0473	.0252	.0168	308.8	247.5	1.103	.02	100.03
13	290.52	76.694	17.09	.0727	.0390	.0165	298.0	251.2	2.604	.05	99.93
15	435.31	172.193	20.60	.1045	.0581	.0518	287.8	249.8	5.846	.11	99.77
17	40.63	1.500	-.00	.1544	.0811	.0513	264.3	268.6	.051	-.00	99.87
19	321.43	93.880	17.97	.1482	.0835	.1233	264.9	269.4	3.187	.06	99.83
21	492.14	220.082	21.67	.1145	.1374	.0905	256.3	241.9	7.472	.14	99.94
23	731.15	485.757	25.10	.2388	.1552	.1290	234.7	237.0	16.491	.30	100.21
25	1276.07	1479.640	29.94	.3783	.2586	.0763	219.6	252.7	50.232	.92	100.22
27	1936.58	3407.850	33.56	.4725	.3067	.2112	207.9	245.7	115.694	2.13	100.02
29	2588.35	6087.749	36.08	.6469	.3662	.3011	191.0	227.9	206.674	3.81	99.25
31	3520.11	11259.589	38.75	.9480	.7586	.5830	171.9	228.3	382.253	7.04	96.92
33	4448.16	17979.194	40.79	1.0208	.4715	.3643	152.5	220.6	610.378	11.24	94.49
35	4821.49	21123.848	41.49	.5007	.3539	.2726	140.6	207.2	717.136	13.21	93.90
37	5355.72	26064.256	42.40	.6483	.3976	.4225	132.6	232.1	884.859	16.30	95.96
38	5415.61	26650.461	42.50	.7548	.4153	.4007	126.9	198.7	904.760	16.66	95.11

T = 1.51471E-09 SEC. NO = 309 STEPS  
TOTAL CAVITY LOSSES = 6436.744 W  
TOTAL SEVER POWER = 173.7 W  
ELECTRONIC EFFIC. = 20.80 PCT  
RESIDUAL BEAM K.E. = 74.31 PCT.

TABLE 7 VA118B-17 GHz

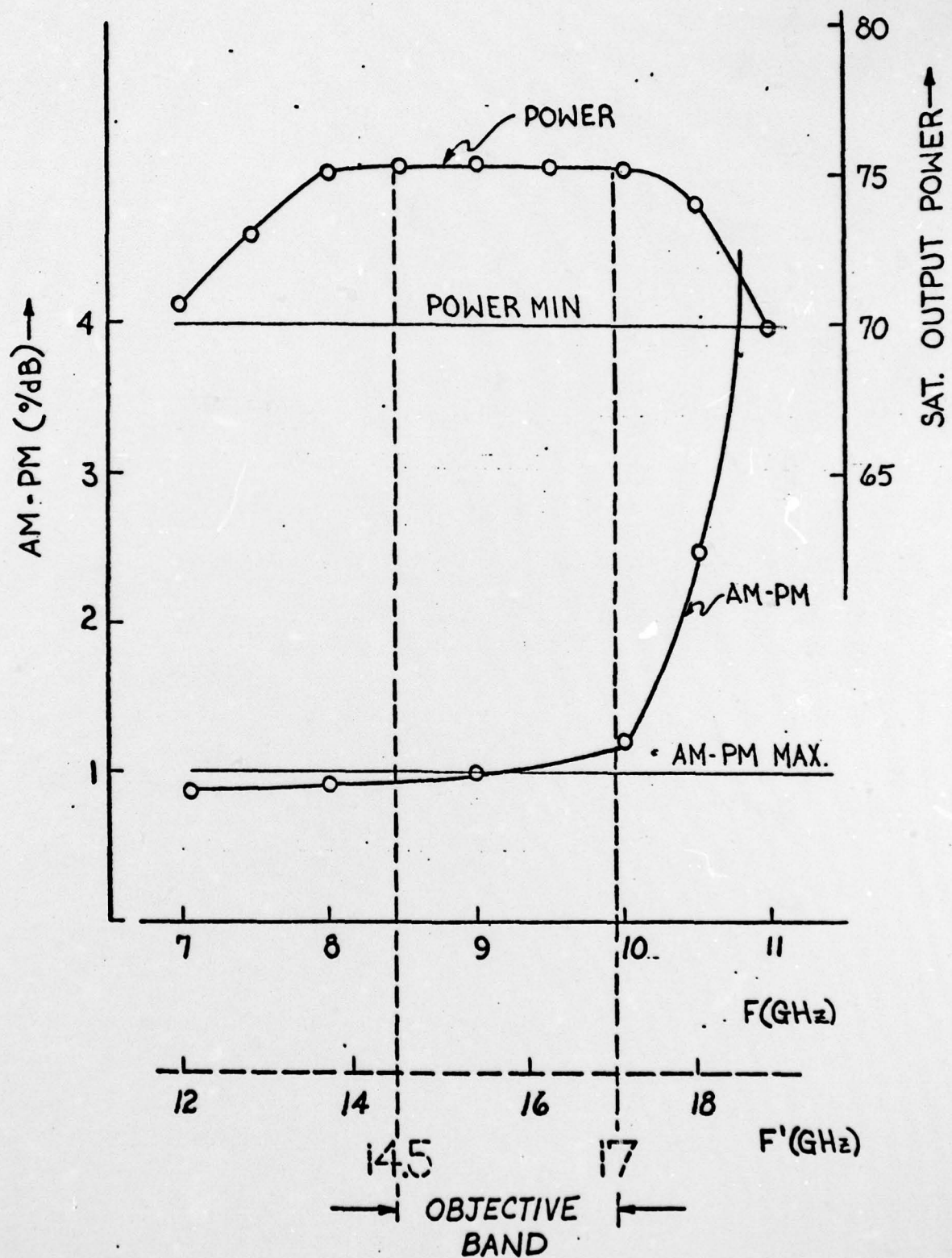


FIG. 24 L-5631 DATA @ 31.5 KV, 6A (DC-200)



in Design 1. This is possible because the AM-PM characteristics are better for the lossy line stabilized tube. This is advantageous because:

- 1) The size of the circuit is maximized making it easier to build and capable of higher average power,
- 2) The similarity is very close to the present 11 - 17 GHz Navy J-Band in that the gun, windows, collector may all be directly used on this tube, and
- 3) The future potential for a full 12 - 18 GHz low AM-PM tube is very good with some improvements in the output section of the tube to extend the present performance to 18 GHz.

The mechanical design for the lossy-line tube is similar to that shown in Figure ~~24~~<sup>25</sup> for the loss button tube. The L-5511 gun, windows and collector will be used directly in this tube.

Construction of the circuit itself is similar to that of the I-Band lossy-line tube. Figure 25 is a drawing of the pole piece used in this tube. The four loss line holes are shown disposed at  $90^\circ$  to one another. Two of the holes are used exclusively for in-band loss, and two are used exclusively for upper cutoff loss. It is necessary to have two in-band loss lines to prevent the large perturbation caused by in-band loading to accumulate in an asymmetric manner. Two upper cutoff lines are advisable to distribute the dissipated power over as much area as possible. The fabrication of the loss lines is also made simpler because each one is coated with only one type of coating. Figure 26 shows the loss coatings used for each type of loss line. The upper cutoff lines use a thin stripe of loss as shown in Figure 26a. This produces a low reference loss and a high "Q" resonance. The in-band coatings are shown in Figure 26b. Here a thicker coating covering the entire circumference is used to produce a high reference loss and a low "Q" resonance.

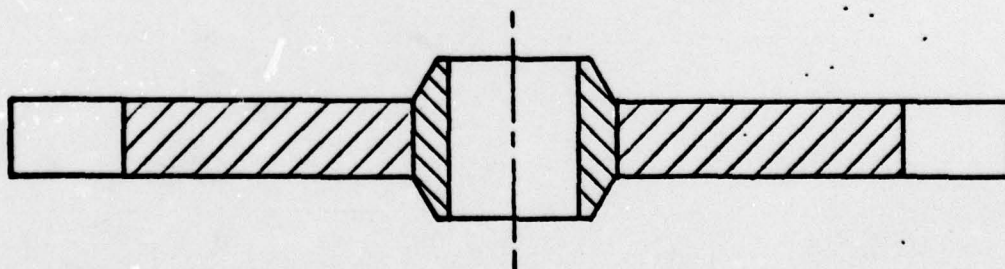
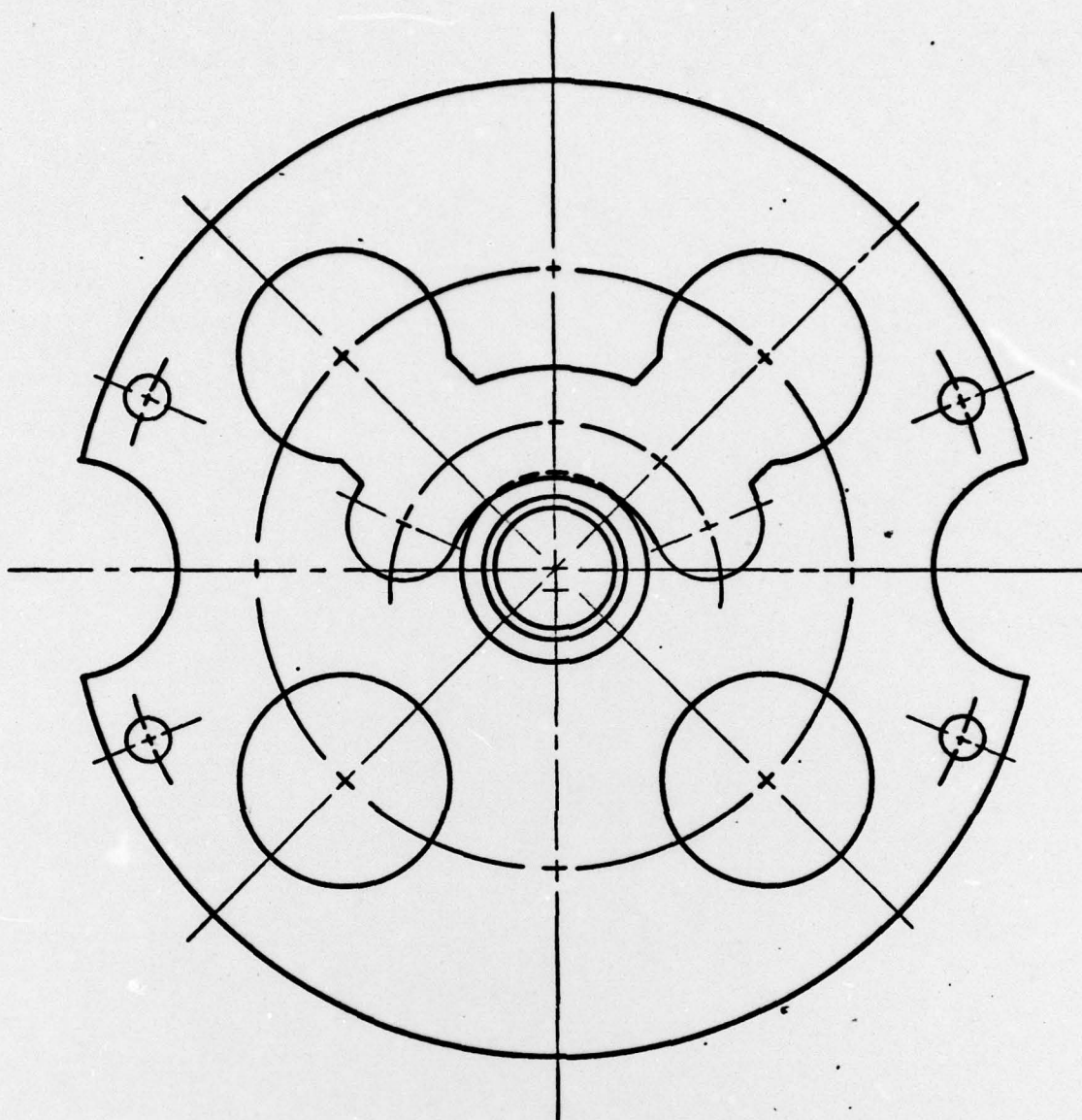


FIG. 25 LOSS - LINE POLE PIECE CONSTRUCTION

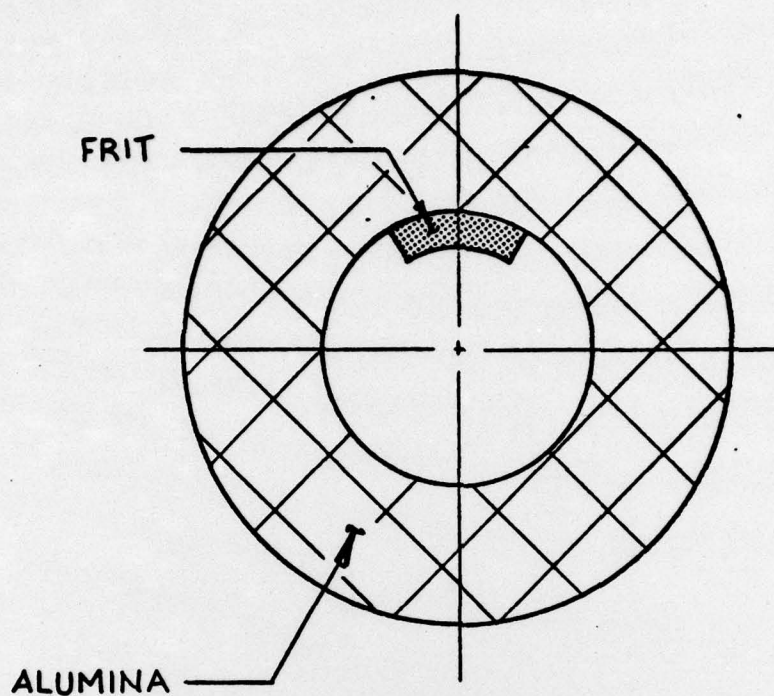


FIG. 26a HIGH "Q" LOSS LINE CONSTRUCTION  
(UPPER CUTOFF)

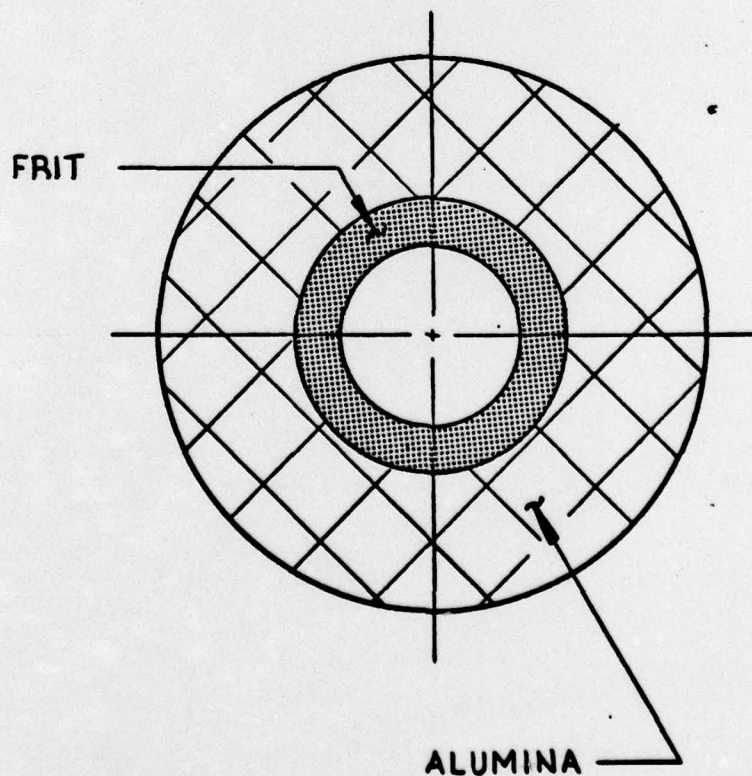


FIG. 26b LOW "Q" LOSS LINE CONSTRUCTION  
(IN-BAND)



Figure 27 shows the match and insertion loss for the output section of S/N 2001. Note that the loss at the low frequency end of the tube is low Q and is spread out from 7.0 to about 10.0 GHz. Note too that the loss rolloff at the high end of the band is sharp or high Q. This is the loss profile needed to stabilize a lossy-line tube.

The circuit layout for the L-5631, S/N 2001 is shown in Figure 28. We expect the layout for the proposed tube to be very similar with some additional cavities added to compensate for the lower small signal gain expected at the lower current design value ( $I_k = 5A$ ). The I-Band design is included here to show how the final design will be approached.

For the layout shown in Figure 28, large signal computer runs were made. The first tube sub-section is an 8-cavity launch section. This section is low loss and nearly unloaded to provide good gain at the band edges of the tube. There is upper cutoff loss to lower the "2 $\pi$ " frequency gain. This section is followed by a heavy attenuator sub-section which when combined with the launch section makes up the input section of the tube. Calculated gain for the input section shows about 24 dB small signal gain with about 6 dB gain variation mostly at the high end of the band. After the input section the loss rods are interrupted by a manifold cavity and the circuit is severed in the conventional manner. This provides 60 - 80 dB isolation between the input and output sections. There are three sub-sections that make up the output section. [A four-cavity lightly attenuated section plus an eight cavity unloaded section combine to provide a 12 cavity low loss power section.] This is essential to achieve the desirable AM-PM and efficiency characteristics at the high end of the band. [The light attenuator cavities are necessary to prevent excessive gain from 7.2 - 8.0 GHz] and to allow some equalization by the heavy output attenuator. The calculated small signal gain of the output section is on the order of 36 dB with a  $\pm 4$  dB variation across the band.

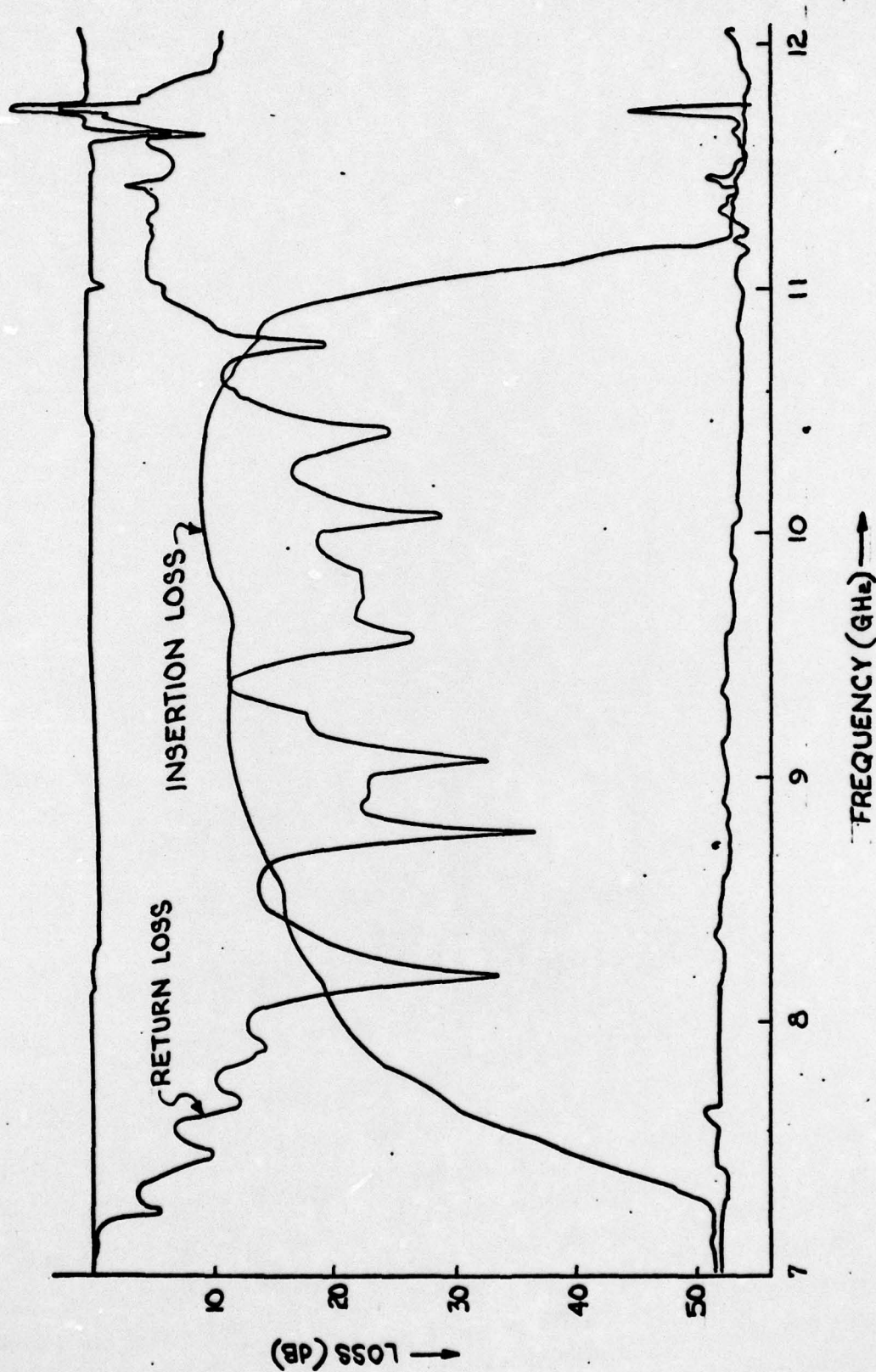


FIG. 27 RETURN LOSS AND INSERTION LOSS FOR THE OUTPUT SECTION AT L-5631, S/N 2001.



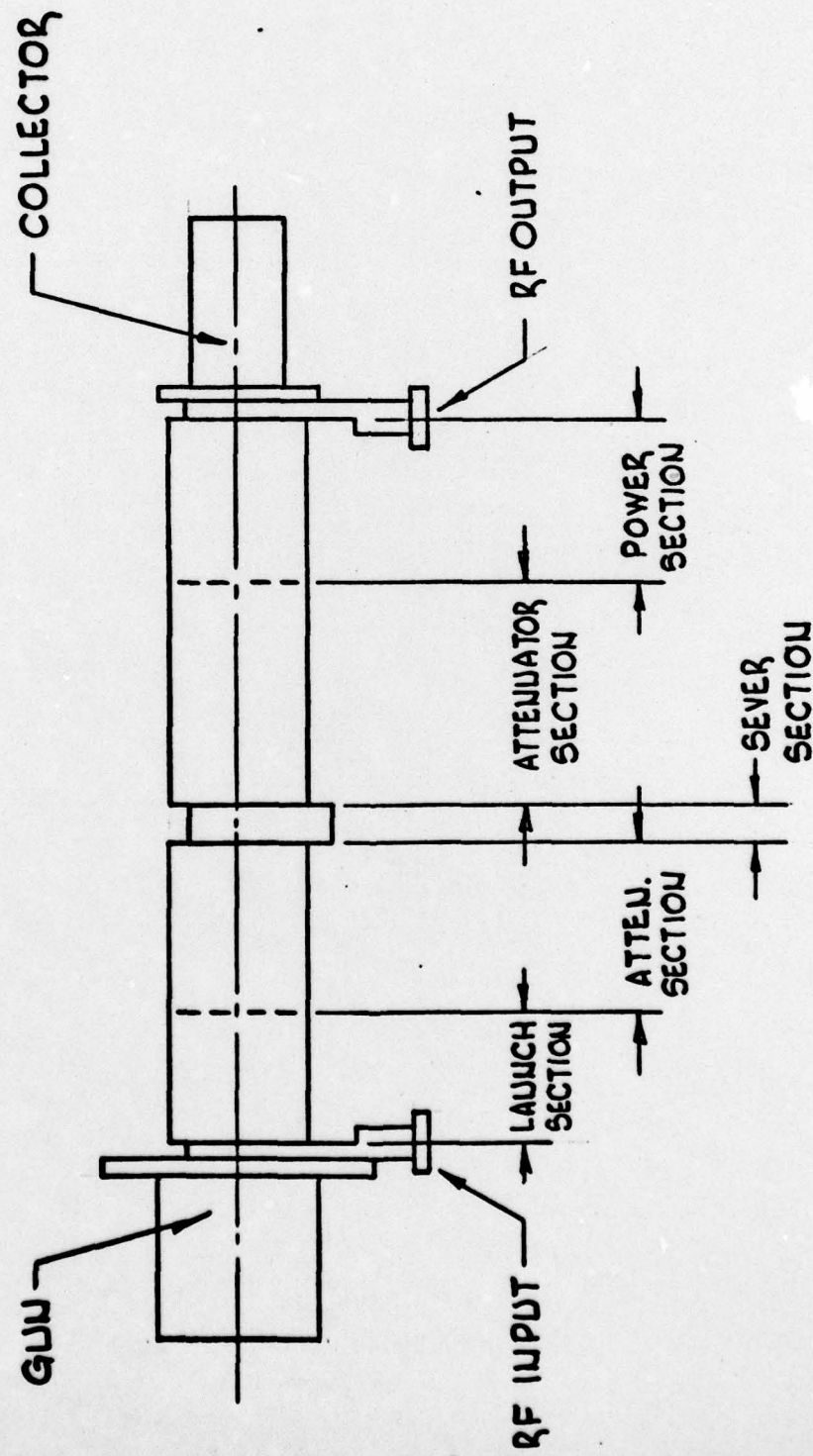


FIG. 28 L-5631 CIRCUIT LAYOUT



The upper cutoff " $2\pi$ " frequency in the loaded section will be about 11.25 GHz. The design loss is 3 dB/Cav. at 11.25 GHz. The upper cutoff loss resonance is designed to be at 11.5 GHz.

The three frequencies chosen for the large signal runs were 7.5 GHz, 9 GHz and 10.5 GHz. The results of the large signal computer run at 7.5 GHz are shown in Figure 29. In the launch section the gain rate is very high but is then sharply reduced in the attenuator region so that the net gain is about 24 dB at the sever. After the sever the gain rate is still curtailed by the attenuator. Even in the power section the gain rate does not increase until the last 8 cavities. The tube saturates at about 20 kW and 56 dB large signal gain. AM-PM at saturation is about  $1.3^\circ/\text{dB}$  as calculated from the 12-disk model.

The computer results at midband (9 GHz) are shown in Figure 30. The effect of the attenuator is smaller at 9 GHz. The gain rate is almost constant throughout the tube. The tube saturates at about 22 kW and a large signal gain of about 49 dB. At saturation the AM-PM calculations show  $1^\circ/\text{dB}$ .

In Figure 31 the computer results at 10.5 GHz are shown. The gain rate is low and some power is transferred outside the power section indicating that it is not quite long enough. The calculated output power is 16 kW and the gain is about 41 dB. At saturation the calculated AM-PM is about  $1.2^\circ/\text{dB}$ .

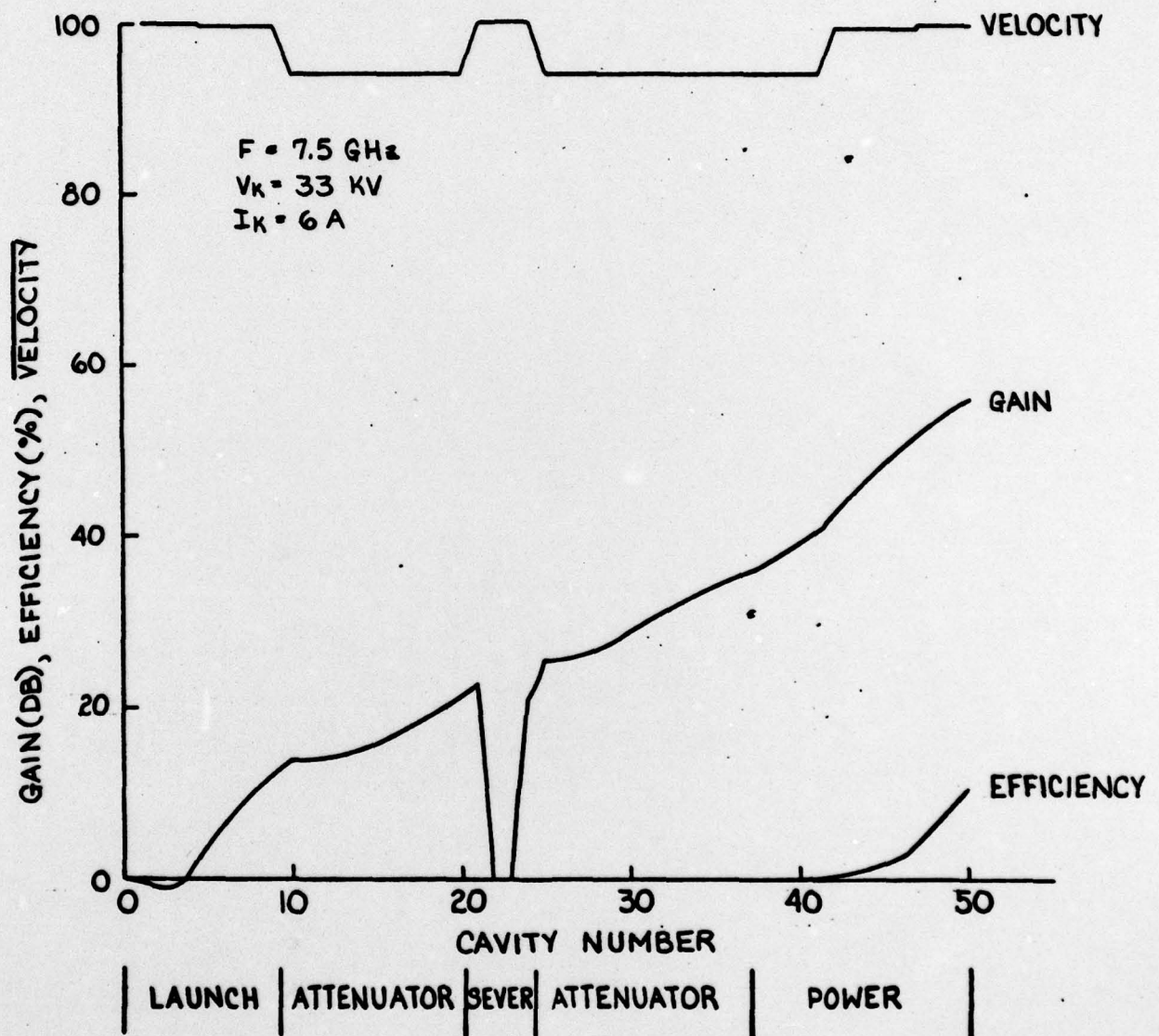


FIG. 29 L-5631 S/N 2001 - 7.5 GHz  
 GAIN, EFFICIENCY, VELOCITY, VS CAVITY NUMBER.



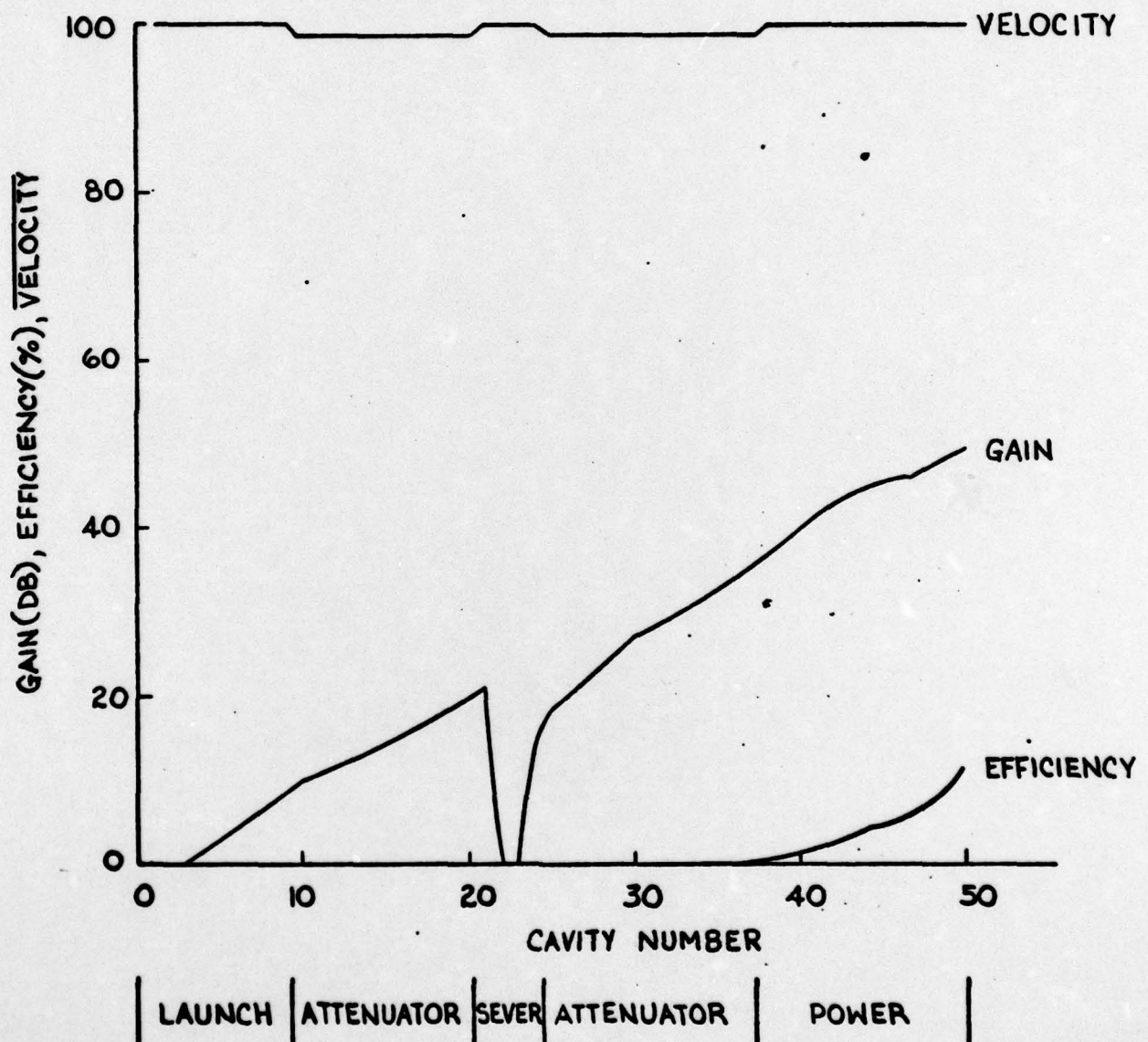


FIG. 30 L-5631 S/N 2001-9.0GHz  
GAIN, EFFICIENCY, VELOCITY, VS. CAVITY NUMBER.



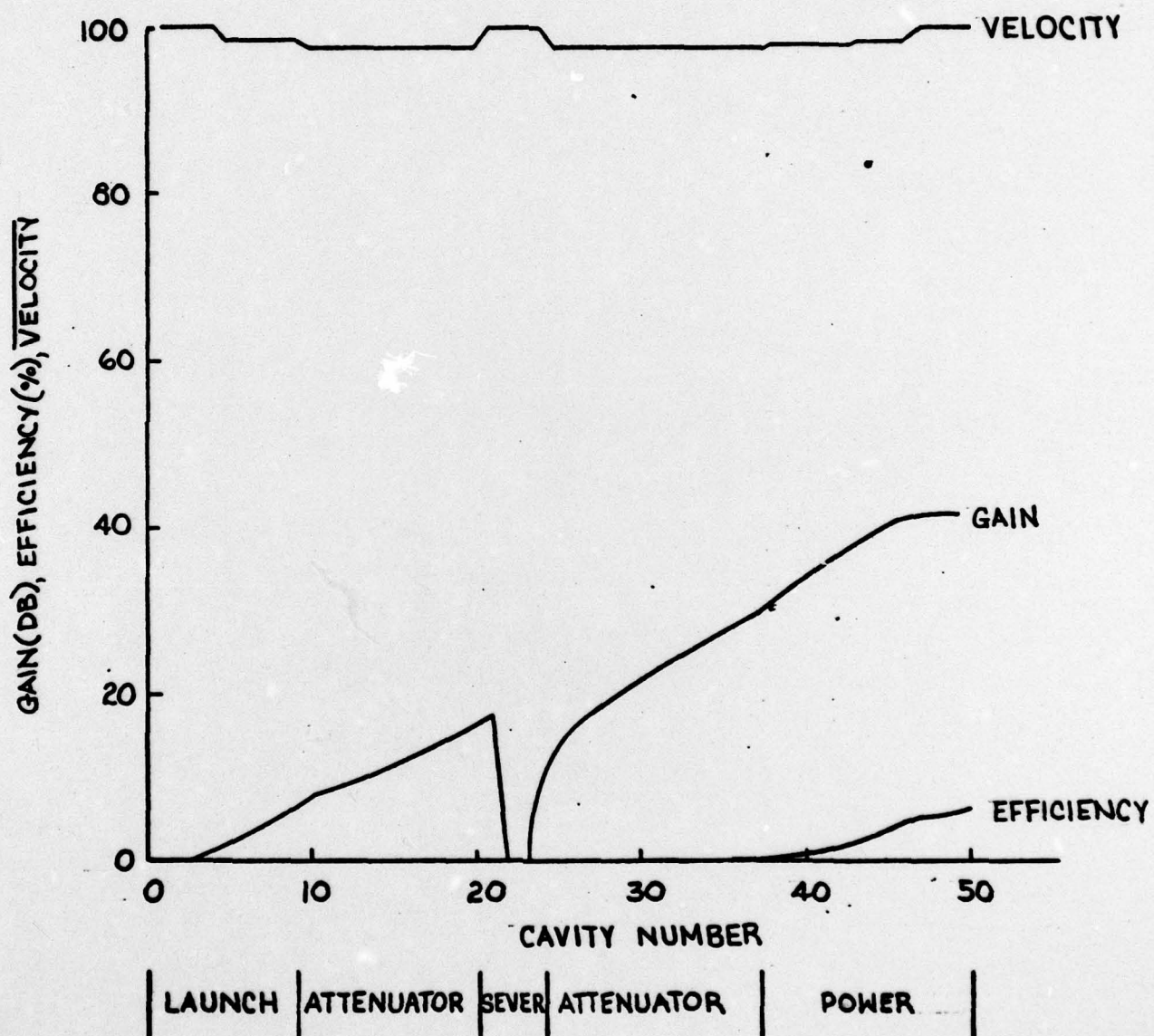


FIG. 31 L-5631 S/N 2001 - 10.5 GHz  
GAIN, EFFICIENCY, VELOCITY, VS. CAVITY NUMBER.

#### 4.0 REFERENCES

1. C. C. Cutler and D. J. Brangaccio, "Factors Affecting Traveling Wave Tube Power Capacity," IRE Trans. on Electron Devices, PGED-3, pp. 9-23 (June 1953).
2. A. Nordsieck, "Theory of large-signal behavior of traveling-wave amplifiers" Proc. IRE, vol 41, pp. 630-637, May, 1953.
3. A. Kiel and P. Parzen, "Nonlinear wave propagation in traveling-wave amplifiers," IRE Trans. Electron Devices, vol ED-2 pp. 26-34, Oct. 1955.
4. P. K. Tien, L. R. Walker and V. W. Wolontis, "A Large Signal Theory of Traveling Wave Amplifiers" Proc. IRE, vol. 43, pp. 260-277 (1955).
5. C. C. Cutler, "The Nature of Power Saturation in Traveling Wave Tubes," BSTJ, Vol. 35, pp. 841-876 (1956).
6. W. R. Beam and D. J. Blattner, "Phase Angle Distortion in Traveling Wave Tubes," RCA Rev., vol. 17, pp. 86-99 (1956).
7. J. P. Laico, H. L. McDowell, and C. R. Moster, "A medium power traveling-wave tube for 6,000 Mc radio relay," Bell Sys. Tech., vol. 35, pp. 1285-1346, 1956.
8. J. E. Rowe, "A large-signal analysis of the traveling-wave amplifier: Theory and general results," IRE Trans. Electron Devices, vol. ED-3, pp. 39-57, Jan. 1956.
9. C. K. Birdsall and C. C. Johnson, "Traveling Wave Tube Efficiency Degradation Due to Power Absorbed in an Attenuator," IRE Trans. on Electron Devices, ED-6, pp. 6-9 (Jan. 1959).
10. A. W. Scott, "Why a Circuit Sever Affects Traveling Wave Tube Efficiency," IRE Trans. on Electron Devices, Vol. ED-9, pp. 35-41 (Jan. 1962).
11. J. Ober, "The Large Signal Behavior of a Traveling Wave Tube With An Attenuating Central Helix Section," Philips Res. Rept., vol. 20, pp. 357-376 (1965).
12. J. I. Lindstrom, "Measurements of Nonlinearities in a Traveling Wave Tube," Internatl. J. Electronics, vol. 21, pp. 425-441 (1966).
13. O. Nilsson, "Nonlinear distortion in traveling-wave tubes," Chalmers Univ. of Tech., Sweden, Research Rep. 67, 1966.
14. A. J. Sangster, "Traveling-wave interactions in structures with nonzero impedance at harmonics of the driving frequency," presented at the 6th Int. Conf. Microwave and Optical Generation and Amplification, Cambridge, England, Sept. 1966.



References (continued)

15. M. E. El-Shandwily and J. E. Rowe, "Multisignal transfer characteristics of a traveling-wave amplifier", Int. J. Electron. vol. 22, no. 5, pp. 461-476, 1967.
16. O. G. Sauseng and U. J. Pittack, "Theoretical and experimental phase distortion in studies on traveling-wave tubes," Hughes Aircraft Co. Tech. Rep. 46, 1969.
17. H. Nishihara and M. Terada, "Effects of Attenuator on the Nonlinear Phase and Distortion of a TWT", IEEE Trans. - Ed., pp. 638-640 (1970).
18. N. J. Dione, "Harmonic generation in octave bandwidth traveling-wave tubes", IEEE Trans. Electron Devices, vol. ED-17, pp. 365-372, Apr. 1970.
19. I. Tanaka and H. Nishihara, "Nonlinear Distortion and Second Harmonics in Traveling-Wave Tubes", Electronics and Communications in Japan, Vol. 55-B, pp. 62-68, 1972.
20. H. Arnett, S. Smith and L. Winslow, "Design Concepts for Dual-Mode TWT," WRL Memorandum Report 2599, Naval Research Laboratory, Wash. D. C. (May 1973).
21. E. Ezura and T. Kano, "Measured and Teoretical Nonlinear Phase Distortion in Traveling-Wave Tubes," IEEE Trans. Electron Devices, vol. ED-22, pp. 890-897, Oct. 1975.
22. J. R. M. Vaughan, "Calculation of Coupled-Cavity TWT Performance" IEEE Trans. on Electron Devices, ED-22, pp. 880-890 (Oct. 1975).